



# Underwater Sound Modeling of Low Energy Geophysical Equipment Operations

---

*Submitted to:*  
CSA Ocean Sciences Inc.  
Stuart, FL  
*Contract:* PSA2389

*Author:*  
Mikhail Zykov

13 September 2013

P001212-001  
Document 00600  
Version 2.0

JASCO Applied Sciences  
Suite 202, 32 Troop Ave.  
Dartmouth, NS B3B 1Z1 Canada  
Phone: +1-902-405-3336  
Fax: +1-902-405-3337  
[www.jasco.com](http://www.jasco.com)



## Document Version Control

Version	Date	Name	Change
1.0	2013 Jun 28	M. Zykov	Version 1 Draft released to client for review.
2.0	2013 Aug 30	M. Zykov	Version 2 released to client.

### Suggested citation:

Zykov, M. 2013. *Underwater Sound Modeling of Low Energy Geophysical Equipment Operations*. JASCO Document 00600, Version 2.0. Technical report by JASCO Applied Sciences for CSA Ocean Sciences Inc.

---

# Contents

---

<b>1. INTRODUCTION .....</b>	<b>1</b>
1.1. Project Description .....	1
1.2. Acoustic Metrics .....	1
<b>2. MODEL METHODOLOGY .....</b>	<b>4</b>
2.1. Source Modeling—Transducer Beam Theory .....	4
2.1.1. Circular Transducers .....	5
2.1.2. Rectangular Transducers .....	6
2.1.3. Multibeam Systems .....	7
2.2. Sound Propagation Modeling .....	8
2.2.1. Two Frequency Regimes: RAM vs. BELLHOP .....	8
2.2.2. N×2-D Volume Approximation .....	8
2.2.3. Sampling of Model Results: Maximum-Over-Depth Rule .....	9
2.2.4. Marine Mammal Frequency Weighting (M-weighting) .....	9
2.3. Acoustic Impact Calculations .....	11
2.3.1. Per-pulse Threshold Distances .....	11
2.3.2. Cumulative Field .....	11
<b>3. MODELING APPROACH.....</b>	<b>12</b>
3.1. Acoustic Sources .....	12
3.1.1. Single Beam Echosounder: Odom CV-100 .....	12
3.1.2. Multibeam Echosounder: R2Sonic 2022 .....	13
3.1.3. Side-scan Sonar: Klein 3000 .....	14
3.1.4. Sub-bottom Profiler: EdgeTech X-Star Sub-bottom Profiler .....	16
3.1.5. Boomer: AP3000 Triple-plate System .....	17
3.2. Scenarios.....	20
3.2.1. Per-pulse Acoustic Field Modeling .....	22
3.2.2. Cumulative Field Modeling.....	22
3.3. Environmental Parameters.....	22
3.3.1. Bathymetry .....	22
3.3.2. Geoacoustics.....	23
3.3.3. Sound Speed Profile .....	24
<b>4. RESULTS.....</b>	<b>26</b>
4.1. Per-pulse Threshold Distances .....	26
4.2. Cumulative Field .....	36

**5. DISCUSSION..... 46**

5.1. Regional Effects of Environmental Parameters on Sound Propagation ..... 46

5.1.1. Effects of Geoacoustic Properties..... 46

5.1.2. Effects of the Sound Speed Profile..... 49

**LITERATURE CITED..... 51**

## Figures

Figure 1. Typical 3-D beam pattern for a circular transducer (Massa 2003). .....	5
Figure 2. Vertical cross section of a beam pattern measured in situ from a transducer used by Kongsberg (source: pers. comm. with the manufacturer). .....	5
Figure 3. Calculated beam pattern for a circular transducer with a beamwidth of 20°. The beam power function is shown relative to the on-axis level using the Robinson projection. ....	6
Figure 4. Calculated beam pattern for a rectangular transducer with a 4° × 10° beamwidth. The beam power function is shown relative to the on-axis level using the Robinson projection. ....	7
Figure 5. Calculated beam pattern for two rectangular transducers engaged simultaneously, with individual beamwidths of 1.5° × 50°, and a declination angle of 25°. The beam power function is shown relative to the on-axis level using the Robinson projection. ....	7
Figure 6. Standard M-weighting for functional marine mammal hearing groups: low-, mid-, and high-frequency cetacean, and pinnipeds in water (Southall et al. 2007). ....	11
Figure 7. Calculated beam pattern vertical slice for the Odom CV-100 single beam echosounder operating at 200 kHz. ....	13
Figure 8. Vertical beam pattern calculated for the R2Sonic 2022 multibeam echosounder with 256 beams of 2° × 2° width in the (left) along- and (right) across-track directions. ....	14
Figure 9. Vertical beam pattern calculated for the Klein 3000 side-scan sonar with two beams of 40° × 1° width in the (left) along- and (right) across-track directions. ....	15
Figure 10. Calculated beam pattern vertical slice for the EdgeTech X-Star sub-bottom profiler at central frequency of 9 kHz. ....	17
Figure 11. Calculated beam pattern vertical slice for the AA202 boomer plate at (a) 1.25 and (b) 16.0 kHz; across-track direction. ....	19
Figure 12. Modeling location overview. ....	21
Figure 13. Sound speed profiles derived from historical monthly average water temperature and salinity (GDEM database) for February, March, April, July, and September. ....	25
Figure 14. <i>Odom CV-100 single beam echosounder</i> : Maximum-over-depth (200 kHz) sound pressure levels around the source. Bathymetry contours (m) are shown in blue. ....	31
Figure 15. <i>R2Sonic 2022 multibeam echosounder</i> : Maximum-over-depth (200 kHz) sound pressure levels around the source. Bathymetry contours (m) are shown in blue. ....	32
Figure 16. <i>Klein 3000 side-scan sonar</i> : Maximum-over-depth (132 kHz) sound pressure levels around the source. Bathymetry contours (m) are shown in blue. ....	33
Figure 17. <i>EdgeTech SBP-216 sub-bottom profiler</i> : Maximum-over-depth (9 kHz) sound pressure levels around the source. Bathymetry contours (m) are shown in blue. ....	34
Figure 18. <i>AP3000 boomer in triple plate configuration</i> : Maximum-over-depth broadband (200–16000 Hz) sound pressure levels around the source. Bathymetry contours (m) are shown in blue. ....	35
Figure 19. Complex scenario for the cumulative sound exposure level (cSEL) acoustic field. Bathymetry contours (m) are shown in blue. ....	38
Figure 20. The sound speed profile analysis locations along the Californian coastline. ....	48

---

## Tables

---

Table 1. Low and high frequency cut-off parameters of M-weighting functions for each marine mammal functional hearing group. ....	11
Table 2. Variable angular steps of the modeling radials in different azimuthal sectors. Steps for the first quadrant (0°–90°) are shown. Steps for the other quadrants are symmetrical. ....	14
Table 3. Variable angular steps of the modeling radials in different azimuthal sectors. Steps for the first quadrant (0°–90°) are shown. Steps for the other quadrants are symmetrical. ....	16
Table 4. Estimated source levels (root-mean-square (rms) sound pressure level (SPL)) and beamwidth from the AR3000 triple-plate boomer operating at 1800 J per pulse distributed into twenty 1/3-octave bands. ....	19
Table 5. Geoacoustic properties of the sub-bottom sediments as a function of depth, in meters below the seafloor (mbsf) for sandy-bottom type. The properties for the sediment layers were derived from the assumed porosity and grain size according to the sediment grain-shearing model (Buckingham 2005). ....	23
Table 6. Geoacoustic properties of the sub-bottom sediments as a function of depth, in meters below the seafloor (mbsf) for hard bottom type. Within each depth range, the parameters vary linearly within the stated range. ....	23
Table 7. <i>Single beam echosounder Odom CV-100 (sandy bottom)</i> : Maximum ( $R_{max}$ , m) and 95% ( $R_{95\%}$ , m) horizontal distances from the source to modeled maximum-over-depth sound level thresholds, with and without M-weighting applied for low-frequency cetaceans (LFC), mid-frequency cetaceans (MFC), high-frequency cetaceans (HFC), and pinnipeds. ....	27
Table 8. <i>Multibeam echosounder R2Sonic 2022 (sandy bottom)</i> : Maximum ( $R_{max}$ , m) and 95% ( $R_{95\%}$ , m) horizontal distances from the source to modeled maximum-over-depth sound level thresholds, with and without M-weighting applied for low-frequency cetaceans (LFC), mid-frequency cetaceans (MFC), high-frequency cetaceans (HFC), and pinnipeds. ....	27
Table 9. <i>Side-scan sonar Klein 3000 (sandy bottom)</i> : Maximum ( $R_{max}$ , m) and 95% ( $R_{95\%}$ , m) horizontal distances from the source to modeled maximum-over-depth sound level thresholds, with and without M-weighting applied for low-frequency cetaceans (LFC), mid-frequency cetaceans (MFC), high-frequency cetaceans (HFC), and pinnipeds. ....	28
Table 10. <i>Side-scan sonar Klein 3000 (exposed bedrock bottom)</i> : Maximum ( $R_{max}$ , m) and 95% ( $R_{95\%}$ , m) horizontal distances from the source to modeled maximum-over-depth sound level thresholds, with and without M-weighting applied for low-frequency cetaceans (LFC), mid-frequency cetaceans (MFC), high-frequency cetaceans (HFC), and pinnipeds. ....	28
Table 11. <i>Sub-bottom profiler EdgeTech X-Star (sandy bottom)</i> : Maximum ( $R_{max}$ , m) and 95% ( $R_{95\%}$ , m) horizontal distances from the source to modeled maximum-over-depth sound level thresholds, with and without M-weighting applied for low-frequency cetaceans (LFC), mid-frequency cetaceans (MFC), high-frequency cetaceans (HFC), and pinnipeds. ....	29
Table 12. <i>Boomer AP3000 triple-plate configuration (sandy bottom)</i> : Maximum ( $R_{max}$ , m) and 95% ( $R_{95\%}$ , m) horizontal distances from the source to modeled maximum-over-depth sound level thresholds, with and without M-weighting applied for low-frequency cetaceans (LFC), mid-frequency cetaceans (MFC), high-frequency cetaceans (HFC), and pinnipeds. ....	29
Table 13. <i>Boomer AP3000 triple-plate system (exposed bedrock bottom)</i> : Maximum ( $R_{max}$ , m) and 95% ( $R_{95\%}$ , m) horizontal distances from the source to modeled maximum-over-depth sound level thresholds, with and without M-weighting applied for low-frequency cetaceans (LFC), mid-frequency cetaceans (MFC), high-frequency cetaceans (HFC), and pinnipeds. ....	30

Table 14. *Multibeam echosounder R2Sonic 2022*: Affected area by specific cumulative sound exposure level (cSEL) thresholds and the approximate distance from the source to modeled maximum-over-depth cumulative thresholds, with and without M-weighting applied for low-frequency cetaceans (LFC), mid-frequency cetaceans (MFC), high-frequency cetaceans (HFC), and pinnipeds. .... 36

Table 15. *Side-scan sonar Klein 3000*: Affected area by specific cumulative sound exposure level (cSEL) thresholds and the approximate distance from the source to modeled maximum-over-depth cumulative thresholds, with and without M-weighting applied for low-frequency cetaceans (LFC), mid-frequency cetaceans (MFC), high-frequency cetaceans (HFC), and pinnipeds. .... 36

Table 16. *Sub-bottom profiler EdgeTech X-Star*: Affected area by specific cumulative sound exposure level (cSEL) thresholds and the approximate distance from the source to modeled maximum-over-depth cumulative thresholds, with and without M-weighting applied for low-frequency cetaceans (LFC), mid-frequency cetaceans (MFC), high-frequency cetaceans (HFC), and pinnipeds. .... 37

Table 17. *Complex scenario*: Affected area by specific cumulative sound exposure level (cSEL) thresholds and the approximate distance from the source to modeled maximum-over-depth cumulative thresholds, with and without M-weighting applied for low-frequency cetaceans (LFC), mid-frequency cetaceans (MFC), high-frequency cetaceans (HFC), and pinnipeds. .... 37

Table 18. Approximate cumulative sound exposure levels for multibeam echosounder, with unweighted and M-weighted radial distances and area ensonified at a pulse rate of 2 pulses per second. ....

Table 19. Approximate cumulative sound exposure levels for multibeam echosounder, with unweighted and M-weighted radial distances and area ensonified at a pulse rate of 4 pulses per second. ....

Table 20. Approximate cumulative sound exposure levels for side-scan sonar, with unweighted and M-weighted radial distances and area ensonified at a pulse rate of 2 pulses per second. ....

Table 21. Approximate cumulative sound exposure levels for side-scan sonar, with unweighted and M-weighted radial distances and area ensonified at a pulse rate of 4 pulses per second. ....

Table 22. Approximate cumulative sound exposure levels for subbottom profiler, with unweighted and M-weighted radial distances and area ensonified at a pulse rate of 2 pulses per second. ....

Table 23. Approximate cumulative sound exposure levels for subbottom profiler, with unweighted and M-weighted radial distances and area ensonified at a pulse rate of 4 pulses per second. ....



---

# 1. Introduction

---

## 1.1. Project Description

An acoustic modeling study was performed to estimate source levels, beam configuration, and sound exposure levels from a set of low energy equipment used in geophysical surveys. The findings of the study will be used for preliminary assessment of the acoustic impact of geophysical surveys planned in the coastal waters of the State of California.

The low energy equipment types covered in the study are:

- Single beam echosounder,
- Multibeam echosounder,
- Side-scan sonar,
- Sub-bottom profiler, and
- Boomer.

The specific models of the equipment considered for the study were suggested by CSA Ocean Sciences Inc. (CSA). The source levels of all equipment, excluding the boomer, were estimated based on the equipment manufacturers' specifications. The source level of the boomer was estimated based on the field measurements conducted by JASCO Applied Sciences Ltd. (JASCO; Martin et al. 2012). The complex beam patterns for each individual instrument were estimated based on beam theory.

The acoustic impact of the survey equipment was assessed based on the distances to the specific thresholds for per-pulse sound pressure levels (SPLs) and sound exposure levels (SELs), as well as cumulative SELs (cSELs). The specific threshold levels in terms of root-mean-square (rms) SPL were 208, 190, 180, 160, 140, and 120 dB re 1  $\mu$ Pa. The specific threshold levels in terms of per-pulse SEL and cSEL were 198, 192, 186, 183, 179, and 171 dB re 1  $\mu$ Pa<sup>2</sup>•s. Based on review comments received on the Draft MND, additional thresholds were added to the results, including 206 dB re 1  $\mu$ Pa SPL and 187 dB re 1  $\mu$ Pa<sup>2</sup>•s SEL to account for more recent fish exposure thresholds of interest (M. Zykov, 2013, pers. comm.).

This report uses a conservative approach. This approach assumes that if there is an uncertainty for a specific modeling input parameter, the value selected from possible range of values is the one that produces higher acoustic impact estimations. The acoustic impact estimations reported in this document should be considered the maximum practically achievable results, rather than the expected average.

The two ocean bottom types most likely to be found in the area of interest were modeled: sandy bottom and exposed bedrock. All five equipment types were modeled in the sandy bottom environment. Only the boomer and side-scan sonar were modeled in the exposed bedrock environment.

## 1.2. Acoustic Metrics

Underwater sound amplitude is measured in decibels (dB) relative to a fixed reference pressure of  $p_0 = 1 \mu$ Pa. Because the loudness of impulsive noise, from the sub-bottom profiler for

example, is not generally proportional to the instantaneous acoustic pressure, several sound level metrics are commonly used to evaluate the loudness of impulsive noise and its effects on marine life.

The zero-to-peak SPL, or peak SPL ( $L_{pk}$ , dB re 1  $\mu$ Pa), is the maximum instantaneous sound pressure level in a stated frequency band attained by an impulse,  $p(t)$ :

$$L_{pk} = 10 \log_{10} \left( \frac{\max(|p^2(t)|)}{p_0^2} \right) \quad (1)$$

The peak SPL metric is commonly quoted for impulsive sounds, but it does not account for the duration or bandwidth of the noise. At high intensities, the peak SPL can be a valid criterion for assessing whether a sound is potentially injurious; however, because the peak SPL does not consider pulse duration, it is not a good indicator of perceived loudness.

The rms SPL ( $L_p$ , dB re 1  $\mu$ Pa) is the rms pressure level in a stated frequency band over a time window ( $T$ , s) containing the pulse:

$$L_p = 10 \log_{10} \left( \frac{1}{T} \int_T p^2(t) dt / p_0^2 \right) \quad (2)$$

The rms SPL can be thought as a measure of the average pressure or as the “effective” pressure over the duration of an acoustic event, such as the emission of one acoustic pulse. Because the window length,  $T$ , is a divisor, pulses more spread out in time have a lower rms SPL for the same total acoustic energy.

In studies of impulsive noise,  $T$  is often defined as the “90% energy pulse duration” ( $T_{90}$ ): the interval over which the pulse energy curve rises from 5% to 95% of the total energy. The SPL computed over this  $T_{90}$  interval is commonly called the 90% rms SPL ( $L_{p90}$ , dB re 1  $\mu$ Pa):

$$L_{p90} = 10 \log_{10} \left( \frac{1}{T_{90}} \int_{T_{90}} p^2(t) dt / p_0^2 \right) \quad (3)$$

The sound exposure level (SEL; dB re 1  $\mu$ Pa<sup>2</sup> s, symbol  $L_E$ ) is a measure of the total acoustic energy contained in one or more pulses. The SEL for a single pulse is computed from the time-integral of the squared pressure over the full pulse duration ( $T_{100}$ ):

$$L_E = 10 \log_{10} \left( \int_{T_{100}} p^2(t) dt / T_0 p_0^2 \right) \quad (4)$$

where  $T_0$  is a reference time interval of 1 s. The SEL represents the total energy (or sound exposure) received over the duration of an acoustic event at some location. The SEL can be a cumulative metric if calculated over time periods containing multiple pulses. The cumulative SEL ( $L_{EC}$ ) can be computed by summing (in linear units) the SELs of the  $n$  individual pulses ( $L_{En}$ ).

$$L_{EC} = 10 \log_{10} \left( \sum_n 10^{\frac{L_{En}}{10}} \right) \quad (5)$$

Because the rms SPL and SEL are both computed from the integral of square pressure, these metrics are related by a simple expression, which depends only on the duration of the 90% energy time window  $T_{90}$ :

$$L_E = L_{p90} + 10\log_{10}(T_{90}) + 0.458 \quad (6)$$

where the 0.458 dB factor accounts for the rms SPL containing 90% of the total energy from the per-pulse SEL.

---

## Model Methodology

---

### **2.1. Source Modeling—Transducer Beam Theory**

Mid- and high-frequency underwater acoustic sources for geophysical measurements create an oscillatory overpressure through rapid vibration of a surface, using either electromagnetic forces or the piezoelectric effect of materials. A vibratory source based on the piezoelectric effect is commonly referred to as a transducer, and may be capable of receiving as well as emitting signals. Transducers are usually designed to produce an acoustic wave of a specific frequency, often in a highly directive beam. The directional capability increases with increasing operating frequency. The main parameter characterizing directivity is the beamwidth, defined as the angle subtended by diametrically opposite “half power” (-3 dB) points of the main lobe (Massa 2003). For different transducers, the beamwidth varies from 180° (almost omnidirectional) to a few degrees.

Transducers are usually built with either circular or rectangular active surfaces. For circular transducers, the beam pattern in the horizontal plane (assuming a downward pointing main beam) is equal in all directions. The beam pattern of a rectangular transducer is variable with the azimuth in the horizontal plane.

The acoustic radiation pattern, or beam pattern, of a transducer is the relative measure of acoustic transmitting or receiving power as a function of spatial angle. Directionality is generally measured in decibels relative to the maximum radiation level along the central axis perpendicular to the transducer surface. The pattern is defined largely by the operating frequency of the device and the size and shape of the transducer. Beam patterns generally consist of a main lobe, extending along the central axis of the transducer, and multiple secondary lobes separated by nulls. The width of the main lobe depends on the size of the active surface relative to the sound wavelength in the medium. Larger transducers produce narrower beams. Figure 1 shows a 3-dimensional (3-D) visualization of a typical beam pattern for a circular transducer.

The true beam pattern of a transducer can be obtained only by in situ measurement of the emitted energy around the device. Such data, however, are not always available, and for propagation modeling it is often sufficient to estimate the beam pattern of the source based on transducer beam theory. An example of a measured beam pattern is shown in Figure 2.

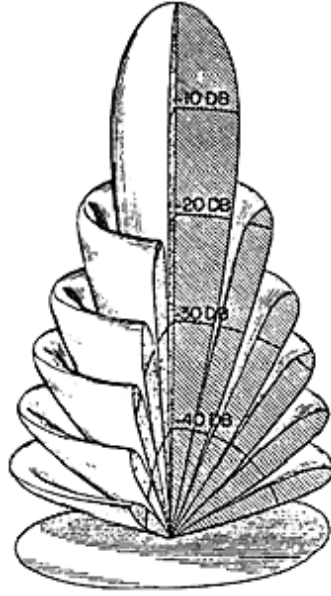


Figure 1. Typical 3-D beam pattern for a circular transducer (Massa 2003).

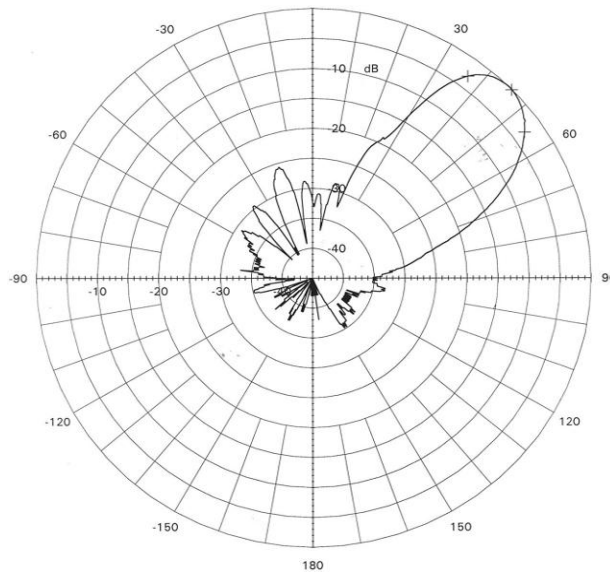


Figure 2. Vertical cross section of a beam pattern measured in situ from a transducer used by Kongsberg (source: pers. comm. with the manufacturer).

### 2.1.1. Circular Transducers

The beam of an ideal circular transducer is symmetrical about the main axis; the radiated level depends only on the depression angle. In this study, beam directivities were calculated from the standard formula for the beam pattern of a circular transducer (Kinsler 1950; ITC 1993). The directivity function of a conical beam relative to the on-axis pressure amplitude is:

$$R(\phi) = \frac{2 \cdot J_1(\pi D_\lambda \sin(\phi))}{\pi D_\lambda \sin(\phi)} \text{ and } D_\lambda = \frac{60}{\theta_{bw}}, \quad (7)$$

where  $J_1$  is the first-order Bessel function,  $D_\lambda$  is the transducer dimension in wavelengths of sound in the medium,  $\theta_{bw}$  is the beamwidth in degrees, and  $\phi$  is the beam angle from the transducer axis. The beam pattern of a circular transducer can be calculated from the transducer's specified beamwidth or from the diameter of the active surface and the operating frequency. The calculated beam pattern for a circular transducer with a beamwidth of  $20^\circ$  is shown in Figure 3. The grayscale represents the source level (dB re 1  $\mu$ Pa @ 1 m) and the declination angle is relative to a central vector ( $0^\circ, 0^\circ$ ) pointing down.

Although some acoustic energy is emitted at the back of the transducer, the theory accounts for the beam power in only the front half-space ( $\phi < 90^\circ$ ) and assumes no energy directed into the back half-space. The relative power at these rearward angles is significantly lower, generally by more than 30 dB, and consequently the emission in the back half-space can be estimated by applying a simple decay rate, in decibels per angular degree, which gives a beam power at  $\phi = 90^\circ$  of 30 dB less than that at  $\phi = 0^\circ$ . This is a conservative estimate of the beam power in the back half-space.

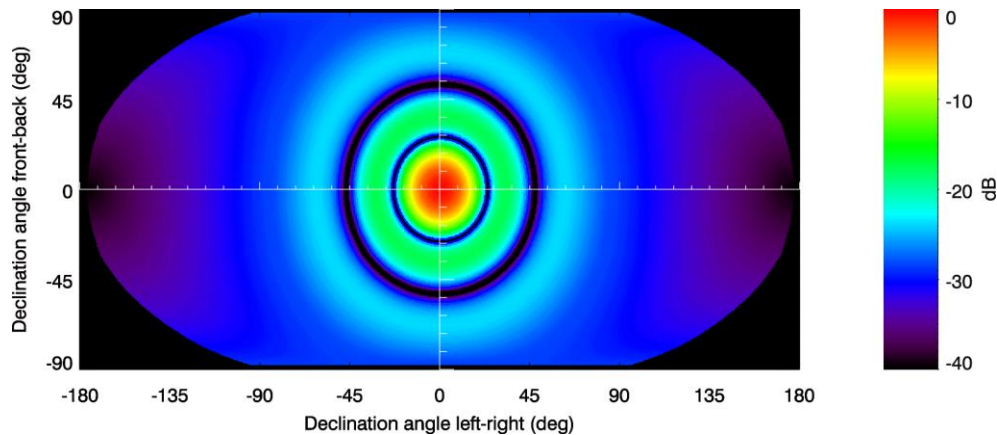


Figure 3. Calculated beam pattern for a circular transducer with a beamwidth of  $20^\circ$ . The beam power function is shown relative to the on-axis level using the Robinson projection.

### 2.1.2. Rectangular Transducers

Rectangular transducer beam directivities were calculated from the standard formula for the beam pattern of a rectangular acoustic array (Kinsler 1950; ITC 1993). This expression is the product of the toroidal beam patterns of two line arrays, where the directional characteristics in the along- and across-track directions are computed from the respective beamwidths. The directivity function of a toroidal beam relative to the on-axis pressure amplitude is:

$$R(\phi) = \frac{\sin(\pi L_\lambda \sin(\phi))}{\pi L_\lambda \sin(\phi)} \quad \text{and} \quad L_\lambda = \frac{50}{\theta_{bw}}, \quad (8)$$

where  $L_\lambda$  is the transducer dimension in wavelengths,  $\theta_{bw}$  is the beamwidth in degrees, and  $\phi$  is the angle from the transducer axis. Here again, the beam pattern of a transducer can be calculated using either the specified beamwidth in each plane or the dimensions of the active surface and the operating frequency of the transducer. The calculated beam pattern for a rectangular transducer with along- and across-track beamwidths of  $4^\circ$  and  $10^\circ$ , respectively, is shown in Figure 4.

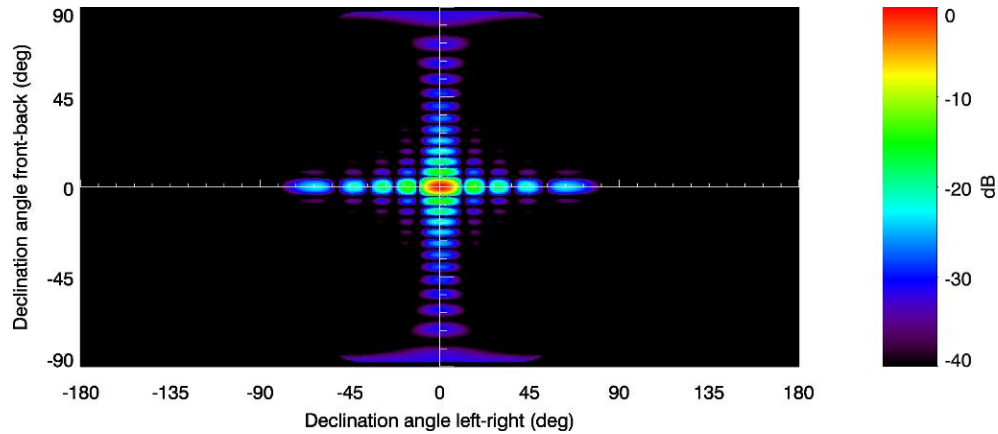


Figure 4. Calculated beam pattern for a rectangular transducer with a  $4^\circ \times 10^\circ$  beamwidth. The beam power function is shown relative to the on-axis level using the Robinson projection.

### 2.1.3. Multibeam Systems

High-frequency systems often have two or more transducers, e.g., side-scan and multibeam sonar. Typical side-scan sonar use two transducers, with the central axes directed perpendicular to the survey track and at some depression angle below the horizontal. In contrast, multibeam bathymetry systems can have upward of 100 transducers. Such systems generally consist of rectangular transducers and have a narrow beamwidth in the horizontal (along-track) plane ( $0.2^\circ\text{--}3^\circ$ ) and a wide beamwidth in the vertical (across-track) plane.

For multibeam systems, the beam patterns of individual transducers are calculated separately and then combined into the overall pattern of the system based on the engagement type of the beams, which can be simultaneous or successive. If the beams are engaged successively, the source level of the system in a given direction is assumed to be the maximum source level realized from the individual transducers; if the beams are engaged simultaneously, the beam pattern of the system is simply the sum of all beam patterns. Figure 5 shows the predicted beam pattern for two rectangular transducers engaged simultaneously. These transducers have along- and across-track beamwidths of  $1.5^\circ$  and  $50^\circ$ , respectively.

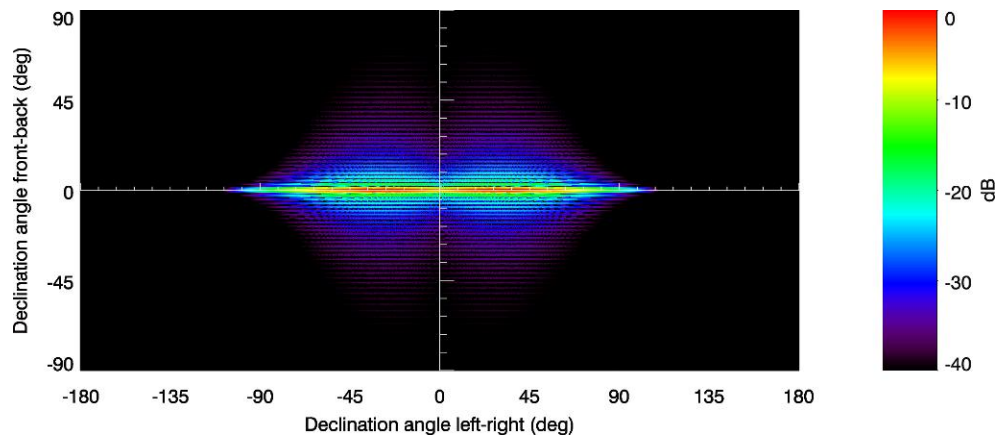


Figure 5. Calculated beam pattern for two rectangular transducers engaged simultaneously, with individual beamwidths of  $1.5^\circ \times 50^\circ$ , and a declination angle of  $25^\circ$ . The beam power function is shown relative to the on-axis level using the Robinson projection.

## 2.2. Sound Propagation Modeling

Underwater sound propagation (i.e., transmission loss) was predicted with JASCO's Marine Operations Noise Model (MONM). This model computes received per-pulse SEL for directional impulsive sources at a specified depth.

### 2.2.1. Two Frequency Regimes: RAM vs. BELLHOP

At frequencies  $\leq 1$  kHz and for omnidirectional sources, MONM computes acoustic propagation via a wide-angle parabolic equation solution to the acoustic wave equation (Collins 1993) based on a version of the U.S. Naval Research Laboratory's Range-dependent Acoustic Model (RAM), which has been modified to account for an elastic seabed. The parabolic equation method has been extensively benchmarked and is widely employed in the underwater acoustics community (Collins et al. 1996). MONM-RAM accounts for the additional reflection loss at the seabed due to partial conversion of incident compressional waves to shear waves at the seabed and sub-bottom interfaces, and it includes wave attenuations in all layers. MONM-RAM's predictions have been validated against experimental data in several underwater acoustic measurement programs conducted by JASCO (Hannay and Racca 2005, Aerts et al. 2008, Funk et al. 2008, Ireland et al. 2009, O'Neill et al. 2010, Warner et al. 2010). MONM-RAM incorporates the following site-specific environmental properties: a modeled area bathymetric grid, underwater sound speed as a function of depth, and a geoacoustic profile based on the overall stratified composition of the seafloor.

At frequencies  $\geq 2$  kHz, MONM employs the widely-used BELLHOP Gaussian beam ray-trace propagation model (Porter and Liu 1994) and accounts for increased sound attenuation due to volume absorption at these higher frequencies following Fisher and Simmons (1977). This type of attenuation is significant for frequencies higher than 5 kHz and cannot be neglected without noticeable effect on model results at long ranges from the source. MONM-BELLHOP accounts for the source directivity, specified as a function of both azimuthal angle and depression angle. MONM-BELLHOP incorporates the following site-specific environmental properties: a bathymetric grid of the modeled area and underwater sound speed as a function of depth. In contrast to MONM-RAM, the geoacoustic input for MONM-BELLHOP consists of only one interface, namely the sea bottom. This is an acceptable limitation because the influence of the sub-bottom layers on the propagation of acoustic waves with frequencies above 1 kHz is negligible.

Both propagation models account for full exposure from a direct acoustic wave, as well as exposure from acoustic wave reflections.

### 2.2.2. $N \times 2$ -D Volume Approximation

MONM computes acoustic fields in three dimensions by modeling transmission loss (via BELLHOP or RAM) within two-dimensional (2-D) vertical planes aligned along radials covering a  $360^\circ$  swath from the source, an approach commonly referred to as  $N \times 2$ -D. These vertical radial planes are separated by an angular step size of  $\Delta\theta$ , yielding  $N = 360^\circ/\Delta\theta$  number of planes. When modeling the acoustic field around the sources with highly directional beam patterns in the horizontal plain (multi-beam or side-scan sonars) a variable angular step size is used. In this case, the step size of about  $1/4$  or  $1/5$  of the beamwidth is selected for the direction

of the main beam to provide representative sampling and greater angular step size for other directions.

MONM treats frequency dependence by computing acoustic transmission loss at the center frequencies of 1/3-octave bands. Sufficiently many 1/3-octave bands, starting at 10 Hz, are modeled to include the majority of acoustic energy emitted by the source. At each center frequency, the transmission loss is modeled via BELLHOP or RAM within each vertical plane ( $N \times 2$ -D) as a function of depth and range from the source. Composite broadband received SELs are then computed by summing the received 1/3-octave band levels. Electromechanical sources generally emit acoustic energy in a narrow frequency band. The width of the band is smaller than the width of 1/3-octave; therefore, the acoustic wave from an electromechanical source can be modeled using a single frequency.

### ***2.2.3. Sampling of Model Results: Maximum-Over-Depth Rule***

The received SEL sound field within each vertical radial plane is sampled at various ranges from the source, generally with a fixed radial step size. At each sampling range along the surface, the sound field is sampled at various depths, with the step size between samples increasing with depth below the surface. The received SEL at a surface sampling location is taken as the maximum value that occurs over all samples within the water column below, i.e., the maximum-over-depth received SEL. This provides a conservative prediction of the received sound level around the source, independent of depth. These maximum-over-depth SELs are presented as color contours around the source.

In principle, the sound field can be sampled at a vertical step size as fine as the acoustic field modeling grid, which varies from 2 m for low frequencies to 6 cm for high frequencies. Such a fine grid of samples, however, would be inefficient and provide a needlessly large quantity of data. The depth spacing between samples is therefore chosen on the basis of the vertical variability of the acoustic field. Vertical variability depends on the variability of the sound speed profile, which is higher at the top of the water column and lower at greater depths. For areas with deep water, sampling is not performed at depths beyond those reachable by marine mammals in the area of interest. At each surface sampling location, the sound field was sampled at the following depths:

- 1, 3 m;
- every 5 m from 5 to 45 m;
- every 10 m from 50 to 90 m;
- every 25 m from 100 to 375 m; and
- every 50 m from 400 to 750 m.

### ***2.2.4. Marine Mammal Frequency Weighting (M-weighting)***

The potential for anthropogenic noise to impact marine species depends on how well the species can hear the sounds produced. Noises are less likely to disturb animals if they are at frequencies that the animal cannot hear well. An exception is when the sound pressure is so high that it can cause physical injury. For non-injurious sound levels, frequency weighting based on audiograms may be applied to weight the importance of sound levels at particular frequencies in a manner

reflective of the receiver's sensitivity to those frequencies (Nedwell and Turnpenny 1998, Nedwell et al. 2007).

Based on a review of literature on marine mammal hearing and on physiological and behavioral responses to anthropogenic sound, Southall et al. (2007) proposed standard frequency-weighting functions—referred to as M-weighting functions—for five functional hearing groups of marine mammals:

- Low-frequency cetaceans (LFC)—mysticetes (baleen whales),
- Mid-frequency cetaceans (MFC)—some odontocetes (toothed whales),
- High-frequency cetaceans (HFC)—odontocetes specialized for using high-frequencies,
- Pinnipeds in water—seals, sea lions and walrus, and
- Pinnipeds in air (not addressed here).

The amount of discount applied by M-weighting functions for less-audible frequencies is less than that indicated by the corresponding audiograms for member species of these hearing groups. The rationale for applying a smaller discount than suggested by audiograms is due in part to an observed characteristic of mammalian hearing that perceived equal loudness curves increasingly have less rapid roll-off outside the most sensitive hearing frequency range as sound levels increase. This is why C-weighting curves for humans, used for assessing loud sounds such as blasts, are flatter than A-weighting curves, used for quiet to mid-level sounds. Additionally, out-of-band frequencies, though less audible, can still cause physical injury if pressure levels are sufficiently high. The M-weighting functions therefore are primarily intended to be applied at high sound levels where impacts such as temporary or permanent hearing threshold shifts may occur. The use of M-weighting should be considered precautionary (in the sense of overestimating the potential for impact) when applied to lower level impacts such as onset of behavioral response. Figure 6 shows the decibel frequency weighting of the four underwater M-weighting functions.

The M-weighting functions have unity gain (0 dB) through the passband and their high and low frequency roll-offs are approximately  $-12$  dB per octave. The amplitude response in the frequency domain of the M-weighting functions is defined by:

$$G(f) = -20 \log_{10} \left[ \left( 1 + \frac{f_{lo}^2}{f^2} \right) \left( 1 + \frac{f^2}{f_{hi}^2} \right) \right] \quad (9)$$

The roll-off and passband of these functions are controlled by the parameters  $f_{lo}$  and  $f_{hi}$ ; the estimated upper and lower hearing limits specific to each functional hearing group (Table 1).

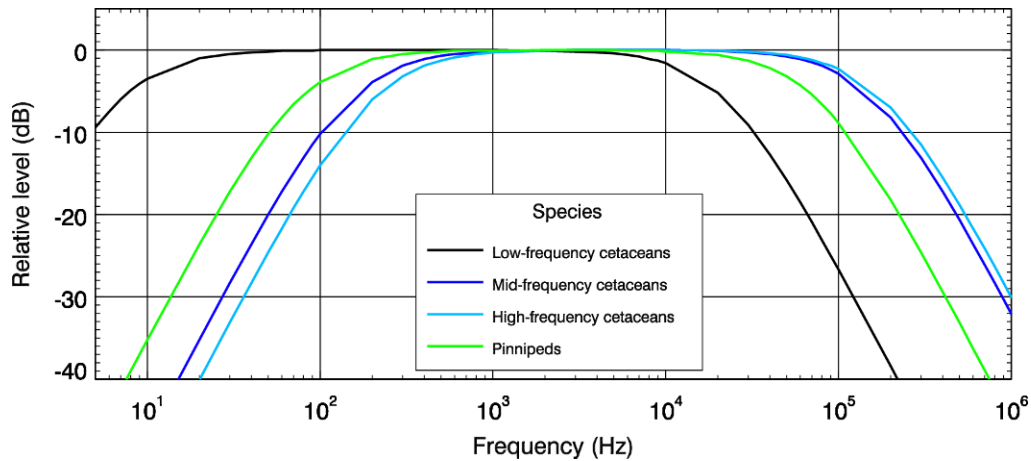


Figure 6. Standard M-weighting for functional marine mammal hearing groups: low-, mid-, and high-frequency cetacean, and pinnipeds in water (Southall et al. 2007).

Table 1. Low and high frequency cut-off parameters of M-weighting functions for each marine mammal functional hearing group.

Functional hearing group	$f_{lo}$ (Hz)	$f_{hi}$ (Hz)
Low-frequency cetaceans	7	22 000
Mid-frequency cetaceans	150	160 000
High-frequency cetaceans	200	180 000
Pinnipeds in water	75	75 000

## 2.3. Acoustic Impact Calculations

### 2.3.1. Per-pulse Threshold Distances

To calculate distances to specified sound level thresholds, the maximum level over all sampled depths was calculated at each horizontal sampling point within the modeled region. The radial grid of maximum-over-depth sound levels was then resampled (by linear triangulation) to produce a regular Cartesian grid (5 m cell size). The contours and threshold ranges were calculated from these flat Cartesian projections of the modeled acoustic fields. To obtain the distances to the specified M-weighted sound level thresholds, the relative level value was applied to the acoustic field modeling frequency (Equation 9).

### 2.3.2. Cumulative Field

To produce maps of cumulative received sound level distribution and to calculate distances to specified sound level thresholds, the maximum level over all sampled depths was calculated at each horizontal sampling point within the modeled region. The radial grids of maximum-over-depth sound levels for each pulse were then resampled (by linear triangulation) to produce a regular Cartesian grid (1 m cell size). The sound field grids from all pulses were summed, using Equation 5, to produce the cumulative sound field grid. The cell size of the grids produced was 50 m. The contours for the specific cSEL thresholds were calculated from these flat Cartesian projections of the modeled acoustic fields. The contours were imported into ESRI ArcGIS software package and the area enclosed by specific contour lines was calculated using internal spatial analysis tools of the package.

---

## Modeling Approach

---

### 3.1. Acoustic Sources

#### 3.1.1. Single Beam Echosounder: Odom CV-100

The representative single beam echosounder system for geophysical survey operations is the Odom CV-100 (manufactured by Teledyne Odom Hydrographic). The standard transducer for this system is the SMSW200-4A. This device's operational frequency is 200 kHz. The sonar head is mounted at the bottom of a ship's hull, with the central axis of the transducer oriented directly downward.

The peak-to-peak source level of the transducer is 230 dB re 1  $\mu$ Pa @ 1 m at 2 kW output power (Airmar 2008). The modeling specifications of the single beam echosounder were:

- Operating frequency: 200 kHz;
- Beam width: 5°;
- Beams: 1;
- Tilt angle (below horizontal plane): 90°;
- Peak-to-peak SPL: 230 dB re 1  $\mu$ Pa @ 1 m;
- rms SPL: 227 dB re 1  $\mu$ Pa @ 1 m;
- Pulse length: 0.1 ms; and
- Per pulse SEL: 187 dB re 1  $\mu$ Pa<sup>2</sup>•s @ 1 m (calculated from available manufacturer specifications).

The Odom CV-100 echosounder was modeled at the single frequency of 200 kHz. Its depth was set to 2 m, based on the assumed draft of the survey vessel. The source beam pattern was modeled using circular transducer theory (Section 2.1.1) assuming 5° beamwidth (Figure 7). The source level was provided in rms SPL units, hence the model output was also in units of rms SPL. The model source level for the echosounder was 230 dB re 1  $\mu$ Pa @ 1 m.

Since echosounder transducers project a circular beam aimed vertically down, the source is effectively omnidirectional in the horizontal plane. A total of 72 radial profiles with equal angular steps of 5° and extending to a maximum range of 5 km from the source were modeled using the MONM-BELLHOP acoustic propagation model (Section 2.2.1).

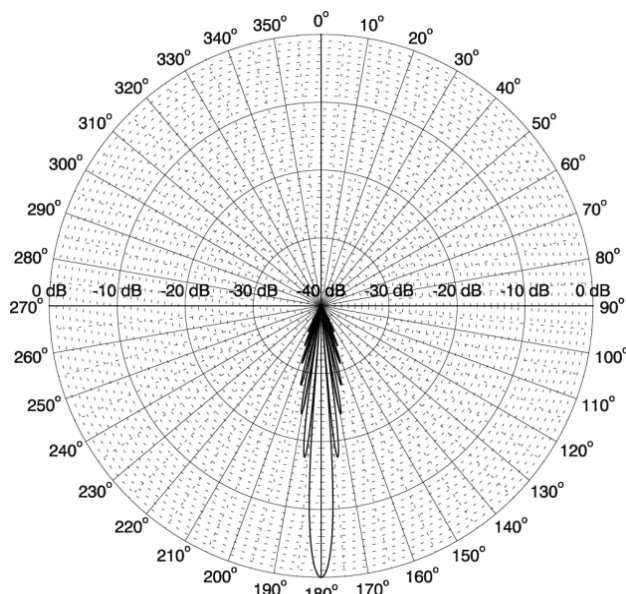


Figure 7. Calculated beam pattern vertical slice for the Odom CV-100 single beam echosounder operating at 200 kHz.

### 3.1.2. Multibeam Echosounder: R2Sonic 2022

The representative multibeam echosounder system for geophysical survey operations is the R2Sonic 2022 (manufactured by R2Sonic, LLC). This device operates at two frequencies: 200 and 400 kHz (R2Sonic 2012). The swath sector is variable from 10° to 160° and is covered by 256 beams. The swath is oriented perpendicular to the tow direction. Each individual beam has a width of 2° × 2° or 1° × 1°, depending on the chosen operational frequency. The sonar head is mounted at the bottom of a ship’s hull.

The adjustable source level of the transducer ranges from 1–221 dB re 1 μPa @ 1 m (R2Sonic 2011). The specifications of the R2Sonic multibeam echosounder system used for the modeling were:

- Operating frequency: 200 kHz and 400 kHz;
- Beam width: 2° × 2°, 1° × 1°;
- Beams: 256;
- rms SPL: 1–221 dB re 1 μPa @ 1 m;
- Pulse length: 0.015–0.5 ms; and
- Per pulse SEL: 173–188 dB re 1 μPa<sup>2</sup>•s @ 1 m (calculated from available manufacturer specifications).

Operational parameters that produce the greatest acoustic impact were modeled. The R2Sonic multibeam echosounder was modeled at the operational frequency of 200 kHz, maximum source level of 221 dB re 1 μPa @ 1 m, the pulse length of 500 μs, and 256 2° × 2° beams covering 160° swath in across-track direction (Figure 8). Its depth was set to 2 m, based on the assumed draft of a survey vessel. The source beam pattern was modeled using rectangular transducer theory (Section 2.1.2) for multibeam systems (Section 2.1.3). The source level was provided in rms SPL units, hence the model output was also in units of rms SPL.

With the R2Sonic 2022's narrow beamwidth, the variability of the emitted energy in the horizontal direction is high. To capture the high variability of the beam in the horizontal plane, a fan of modeling radials with variable angular step size was created (Table 2). The density of the radials was greater in the source's broadside direction, where beam variability is at its maximum, and lesser in the endfire direction. A total of 660 radials were modeled using the MONM-BELLHOP acoustic propagation model (Section 2.2.1). The source heading was in-line with the vessel track. The maximum range of modeling was 10 km from the source.

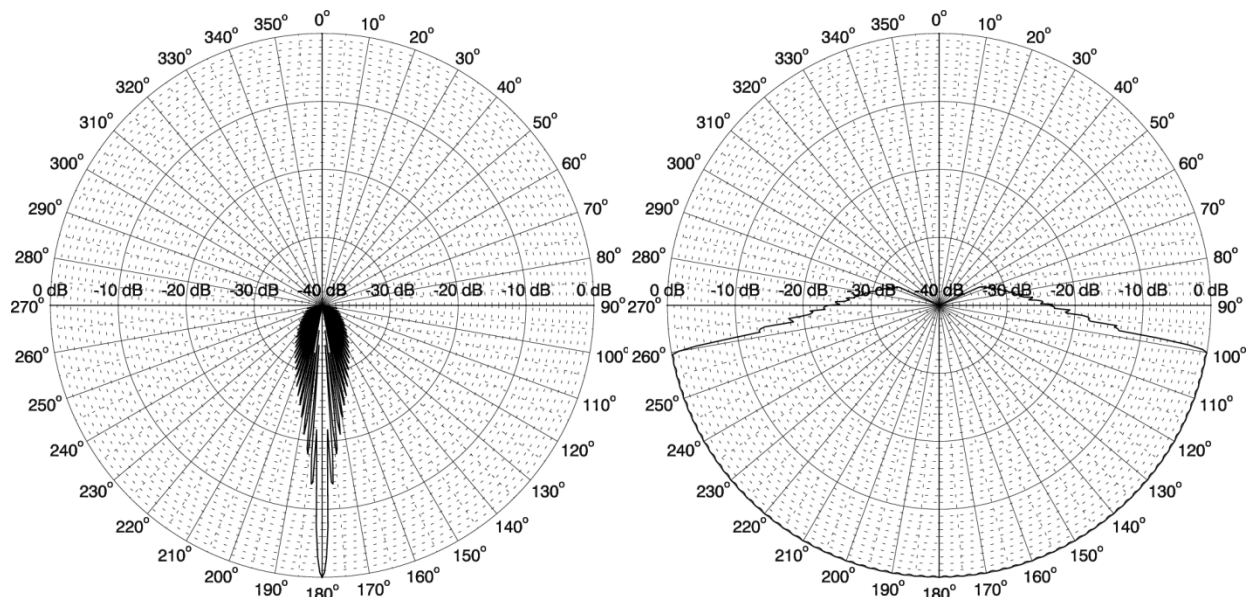


Figure 8. Vertical beam pattern calculated for the R2Sonic 2022 multibeam echosounder with 256 beams of  $2^\circ \times 2^\circ$  width in the (left) along- and (right) across-track directions.

Table 2. Variable angular steps of the modeling radials in different azimuthal sectors. Steps for the first quadrant (0–90°) are shown. Steps for the other quadrants are symmetrical.

Azimuth	Angular step, $\Delta\theta$
0–45°	1°
45–80°	0.5°
80–90°	0.2°

### 3.1.3. Side-scan Sonar: Klein 3000

The representative side-scan sonar system for geophysical survey operations is the Klein 3000 (manufactured by Klein Associates, Inc.). This device operates at two frequencies: 132 and 500 kHz (L-3 Klein Associates 2010). The sonar projects two beams in the broadside directions. The tilt angle of the beam is variable  $5^\circ$ – $20^\circ$  down from the horizontal plane. The beams are  $40^\circ \times 1^\circ$  width. The sonar is mounted on a tow-fish. The source level of the sonar is 234 dB re 1  $\mu$ Pa @ 1 m at 132 kHz (Hydro International 2010). The specifications of the Klein 3000 side-scan sonar used for the modeling were:

- Operating frequency: 132 kHz;
- Beam width:  $40^\circ \times 1^\circ$ ;

- Beams: 2;
- Tilt angle (below horizontal plane): 5°;
- rms SPL: 234 dB re 1 μPa @ 1 m;
- Pulse length: 0.4 ms; and
- Per pulse SEL: 200 dB re 1 μPa<sup>2</sup>•s @ 1 m (calculated from available manufacturer specifications).

The Klein 3000 side-scan sonar was modeled at a single frequency of 132 kHz. Its depth was set to 3 m, based on the assumed tow depth of a tow-fish. The source beam pattern was modeled using rectangular transducer theory (Section 2.1.1) assuming 40° × 1° (across- and along-track) beamwidth (Figure 9). The source level was provided in rms SPL units, hence the model output was also in units of rms SPL. The model source level for the echosounder was 234 dB re 1 μPa @ 1 m.

With the Klein 3000’s narrow beamwidth, the variability of the emitted energy in the horizontal direction is high. To capture the high variability of the beam in the horizontal plane, a fan of modeling radials with variable angular step size was created (Table 3). The density of the radials was greater in the source’s broadside direction, where beam variability is at its maximum, and lesser in the endfire direction. A total of 660 radials were modeled using the MONM-BELLHOP acoustic propagation model (Section 2.2.1). The source heading was assumed in-line with a survey vessel’s track. The maximum range of modeling was selected to be 10 km from the source.

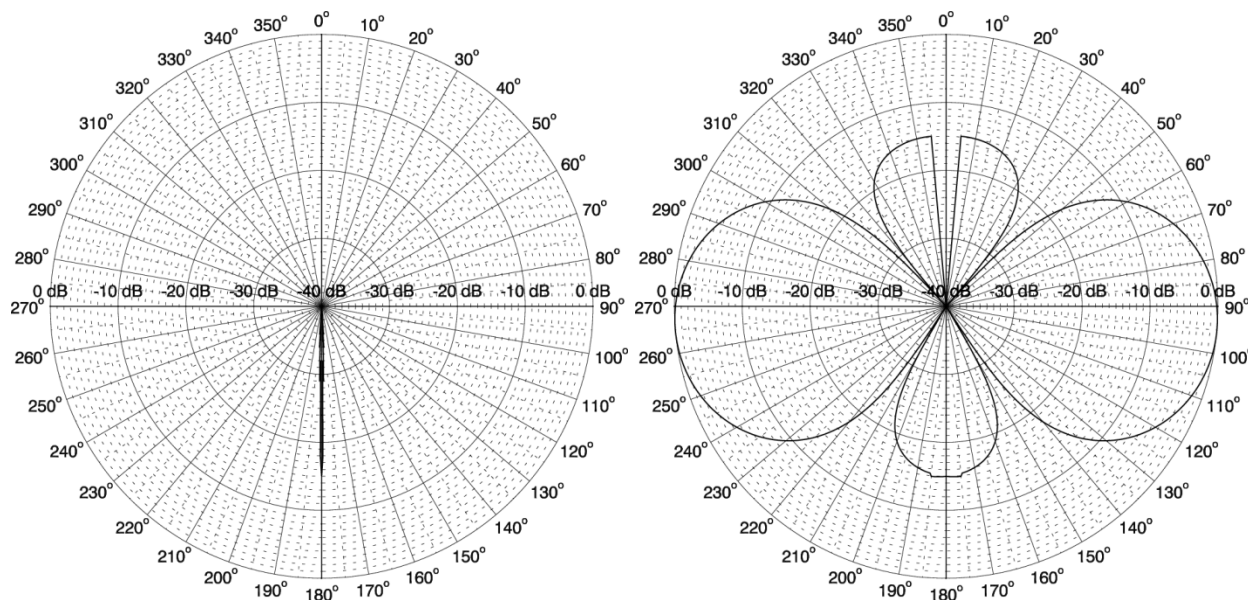


Figure 9. Vertical beam pattern calculated for the Klein 3000 side-scan sonar with two beams of 40° × 1° width in the (left) along- and (right) across-track directions.

Table 3. Variable angular steps of the modeling radials in different azimuthal sectors. Steps for the first quadrant (0–90°) are shown. Steps for the other quadrants are symmetrical.

Azimuth	Angular step, $\Delta\theta$
0–45°	1°
45–80°	0.5°
80–90°	0.2°

### 3.1.4. Sub-bottom Profiler: EdgeTech X-Star Sub-bottom Profiler

The representative sub-bottom profiler system for geophysical survey operations is the EdgeTech X-Star (manufactured by EdgeTech). The system is equipped with a SBP-216 tow-fish. The transducer installed on the SBP-216 tow-fish transmits a chirp pulse that spans an operator-selectable frequency band. The lower and upper limits of the sonar's frequency band are 2 and 16 kHz, respectively. The system projects a single beam directed vertically down. The projected beamwidth depends on the operating frequency, and it can vary in range from 17° to 24°. The source level of the profiler is 210 dB re 1  $\mu$ Pa @ 1 m.

The specifications of the EdgeTech X-Star sub-bottom profiler system used for the modeling were:

- Operating frequency: 9 kHz;
- Beam width: 24°;
- Beams: 1;
- Tilt angle (below horizontal plane): 90°;
- rms SPL: 210 dB re 1  $\mu$ Pa @ 1 m;
- Pulse length: 20 ms; and
- Per pulse SEL: 193 dB re 1  $\mu$ Pa<sup>2</sup>•s @ 1 m (calculated from available manufacturer specifications).

The EdgeTech X-Star was modeled at a single frequency of 9 kHz that represents the central frequency of the usable band. Its depth was set to 3 m, based on the assumed tow depth of a tow-fish. The source beam pattern was modeled using circular transducer theory (Section 2.1.1) assuming a 24° beamwidth (Figure 10). The source level was provided in rms SPL units, hence the model output was also in units of rms SPL. The model source level for the echosounder was 210 dB re 1  $\mu$ Pa @ 1 m.

Since the echosounder's transducer projects a circular beam that is aimed vertically down, the source is effectively omnidirectional in the horizontal plane.

A total of 72 radial profiles with equal angular step of 5° and extending to a maximum range of 10 km from the source were modeled using the MONM-BELLHOP acoustic propagation model (Section 2.2.1).

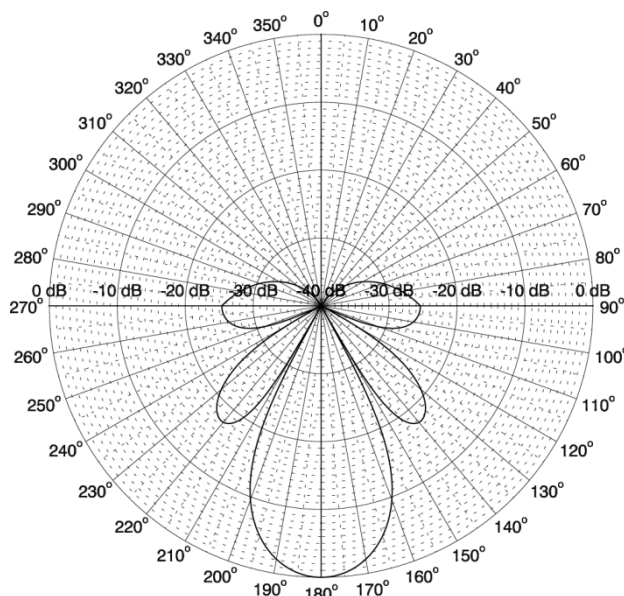


Figure 10. Calculated beam pattern vertical slice for the EdgeTech X-Star sub-bottom profiler at central frequency of 9 kHz.

### 3.1.5. Boomer: AP3000 Triple-plate System

The representative boomer system for geophysical survey operations is the AP3000 triple-plate boomer (manufactured by Subsea Systems, Inc.). In order to produce estimates of the sound field for the boomer source, the specifications of the Applied Acoustics AA202 boomer plate were taken to represent a single plate, three of which comprise the full system. The boomer plate is 38 cm wide by 38 cm long with a circular baffle. Because the boomer source is a circular piston surrounded by a rigid baffle, it cannot be considered a point-like source (Verbeek and McGee 1995). The beam pattern of a boomer plate shows some directivity for frequencies above 1 kHz. Above this frequency, the acoustic wave's emitted length becomes comparable (of the same order of magnitude) with the baffle size (< 150 cm vs. 35 cm).

The input energy for the AP3000 system is up to 600 J per pulse per plate, or up to 1800 J per pulse from all three plates. The width of the pulse calculated based on the 90% rms SPL is 0.2 ms.

JASCO performed a source verification study on an AP3000 system (Martin et. al 2012) with a double-plate configuration operating at maximum input energy of 1000 J. During the study, the acoustic data were collected as close as 8 m to the source and directly below it. The data showed that the broad band source level for the system was 203.3 dB  $1 \mu\text{Pa}$  @ 1 m rms SPL over 0.2 ms window length and 172.6 dB re  $1 \mu\text{Pa}^2 \cdot \text{s}$  @ 1 m SEL. The field data also revealed that even at 10 m from the source the  $T_{90}$  is significantly longer than 0.2 ms: for distances from 8 to 20 m from the source the  $T_{90}$  varied from 6 ms to 10 ms and for distances more than 20 m the  $T_{90}$  was greater than 10 ms.

The increase in the source level of an AR3000 boomer when in triple-plate configuration, instead of double-plate configuration, was estimated at 2.6 dB because a triple-plate configuration could be used with a higher energy input per pulse (up to 1800 J vs. up to 1000 J for double plate configuration). For modeling, the source level of the AR3000 triple-plated boomer operating at

1800 J per pulse energy was considered to be 205.9 dB  $1 \mu\text{Pa}$  @ 1 m rms SPL over 0.2 ms window length and 175.6 dB re  $1 \mu\text{Pa}^2 \cdot \text{s}$  @ 1 m SEL.

The power spectrum of the boomer signal and the beamwidth at different frequencies was estimated based on Simpkin's (2005) study of the Hunttec'70 Deep Tow Boomer, a typical boomer plate of comparable dimensions. The source level in each 1/3-octave band was calculated based on the broad band source level and relative power spectrum data (Table 4).

The beamwidth of a boomer plate at each 1/3-octave frequency was calculated based on the standard formula for the beam pattern of a circular transducer (Equation 7). Figure 11 shows a vertical slice for the calculated beam pattern at (a) 1.25 and (b) 16.0 kHz. In order to simplify the acoustic propagation calculations, the beam pattern from the triple-plate system was considered to be equal to the beam pattern from a single plate.

The boomer source can be treated as an omnidirectional source for the frequencies of 1000 Hz and lower. For frequencies higher than 1000 Hz, the directionality of the boomer was taken into account. The acoustic field projected by the boomer source was modeled using two propagation models: for frequencies of 1000 Hz and below MONM-RAM was used, while frequencies above 1000 Hz were modeled using MONM-BELLHOP.

The acoustic propagation modeling was conducted in terms of SEL units. The conversion to the rms SPL units was done based on Equation 6 considering the  $T_{90}$  equal to 0.2 ms for the distances from the source less than 20 m, and 10 ms for the distances greater than 20 m from the source.

The specifications of the AR3000 triple-plate boomer system used for the modeling were:

- Operating frequency (broad band): 200 Hz–16 kHz;
- Beam width: omnidirectional  $-8^\circ$ ;
- Beams: 1;
- Tilt angle (below horizontal plane):  $90^\circ$ ;
- Maximum energy input (per shot): 1800 J;
- rms SPL: 205.9 dB re  $1 \mu\text{Pa}$  @ 1 m (estimated from field measurements; Martin et al. 2012);
- Pulse length: 0.2 ms; and
- Per pulse SEL: 175.6 dB re  $1 \mu\text{Pa}^2 \cdot \text{s}$  @ 1 m (estimated from field measurements; Martin et al. 2012).

Table 4. Estimated source levels (root-mean-square (rms) sound pressure level (SPL)) and beamwidth from the AR3000 triple-plate boomer operating at 1800 J per pulse distributed into twenty 1/3-octave bands.

Third-octave band center frequency (Hz)	rms SPL (over 0.2 ms window; dB re 1 $\mu$ Pa at 1 m)	SEL (dB re 1 $\mu$ Pa <sup>2</sup> ·s at 1 m)	Beam width
200	189.9	158.0	omnidirectional
250	190.3	158.4	omnidirectional
315	191.0	159.1	omnidirectional
400	191.6	159.7	omnidirectional
500	192.4	160.5	omnidirectional
630	193.3	161.4	omnidirectional
800	193.9	162.0	omnidirectional
1,000	194.7	162.8	omnidirectional
1,250	195.4	163.5	105°
1,600	195.5	163.6	78°
2,000	195.8	163.9	60°
2,500	195.3	163.4	47°
3,150	194.7	162.8	37°
4,000	194.0	162.1	29°
5,000	192.8	160.9	23°
6,400	191.7	159.8	18°
8,000	190.0	158.1	14°
10,000	186.7	154.8	11°
12,800	180.7	148.8	9°
16,000	170.7	138.8	8°
Broadband	205.9	174.0	

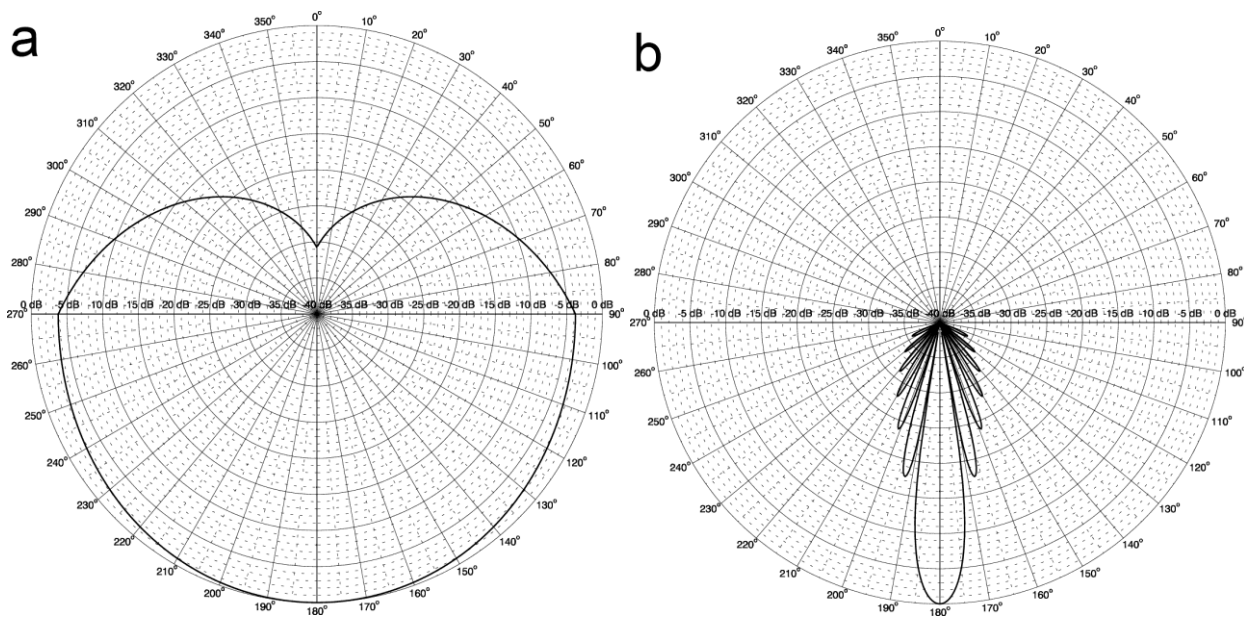


Figure 11. Calculated beam pattern vertical slice for the AA202 boomer plate at (a) 1.25 and (b) 16.0 kHz; across-track direction.

### **3.2. Scenarios**

The results of the modeling presented in this report will be used as the reference for planning of a geophysical survey using low energy high-frequency survey equipment. The representative modeling location was chosen off the coast of the San Luis Obispo County, CA near the Diablo Canyon Power Plant. The geophysical surveys will be performed inside the State Seward Boundary (SSB) that extends 3 nmi from the shoreline.

Five low energy survey instruments were selected for modeling:

1. Single beam echosounder: Odom CV-100;
2. Multibeam echosounder: R2Sonic 2022;
3. Side-scan sonar: Klein 3000;
4. Sub-bottom profiler: EdgeTech X-Star with tow-fish SBP-216; and
5. Boomer: AP3000 triple-plate configuration.

The acoustic field from the sources was evaluated in terms of per-pulse rms SPL and SEL metrics, as well as cSEL. The cSEL field was estimated for each instrument operated individually along three lines (Figure 12). Also, a complex survey scenario was considered, for which a combined cSEL field was estimated from several instruments.

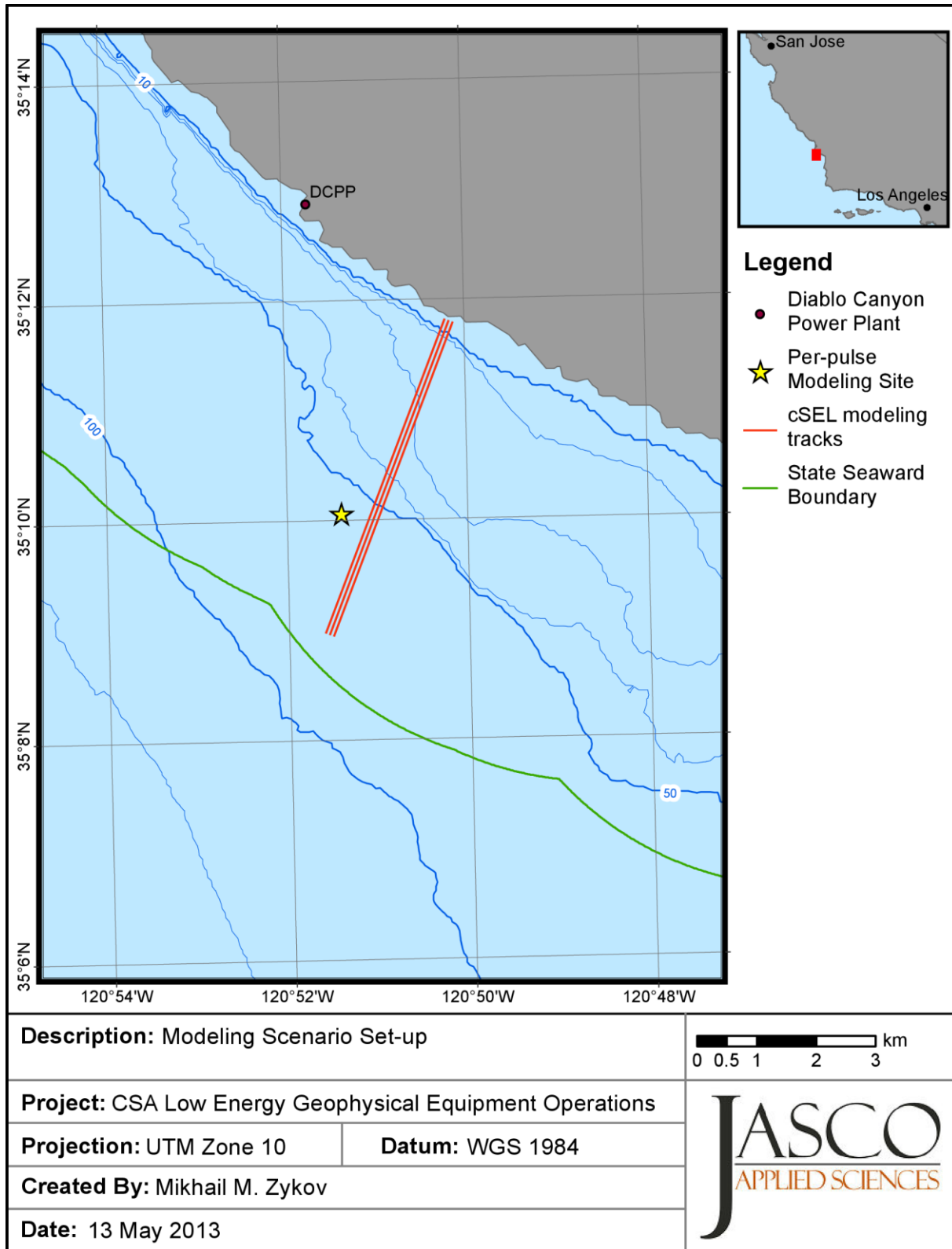


Figure 12. Modeling location overview.

### 3.2.1. Per-pulse Acoustic Field Modeling

The modeling site for the per-pulse acoustic field modeling was selected within the 3 nmi offshore zone. The water depth at the site is 64 m (Figure 12).

The sound fields for single impulses from the five survey instruments were modeled in  $N \times 2$ -D mode up to 50 km using a horizontal angular resolution of  $5^\circ$  (72 radials) for horizontally omnidirectional sources and up to 660 radials with variable angular resolution for narrow beam instruments. The horizontal distance was 10 m between receiver points. The selected maximum modeling distance was sufficient to fully enclose the 120 dB re 1  $\mu$ Pa rms SPL threshold.

The two bottom types most likely to be found in the area of interest were modeled: sandy bottom and exposed bedrock. All five equipment types were modeled in the sandy bottom environment. Only the boomer and side-scan sonar were modeled in the exposed bedrock environment.

### 3.2.2. Cumulative Field Modeling

Six cumulative sound field scenarios were modeled: one per individual survey instrument plus a complex scenario. Each scenario estimates an aerial distribution of the cSEL using a representative track configuration: three parallel lines 75 m from each other. The lines are oriented perpendicular to the shoreline and extend from the shallowest waters the vessel can operate in ( $\sim 5$  m water depth) to the outer limit of the 3 nmi offshore zone. The length of each survey line was about 5.7 km.

The assumed operational speed of the vessel along the survey lines was 4 knots ( $\sim 2$  m/s). The time required to complete the three-line survey is approximately 2.5 hr, including the line change. The assumed pulse rate was one pulse every 4 s. Considering the anticipated vessel speed, the horizontal separation between the pulses would be approximately 8 m.

The complex scenario for the cumulative field modeling consists of a survey with two instruments operating simultaneously and with one repeated line:

- Multibeam echosounder + sub-bottom profiler: three lines;
- Multibeam echosounder + sub-bottom profiler: one center line (re-shooting);
- Multibeam echosounder + side-scan sonar: three lines; and
- Multibeam echosounder + side-scan sonar: one center line (re-shooting).

The total length of the track lines for the complex scenario is 45.6 km. The estimated time to complete the course of the complex scenario is about 6.5 hr.

## 3.3. Environmental Parameters

### 3.3.1. Bathymetry

The bathymetry data was extracted from the National Geophysical Data Center (NGDC) U.S. Coastal Relief Model (NGDC 2003). These bathymetry data, with a resolution of 3 arc-seconds (about  $75 \times 90$  m), extend up to about 200 km from the U.S. coast.

### 3.3.2. Geoacoustics

MONM assumes a single geoacoustic profile of the seafloor for the entire modeled area. The acoustic properties required by MONM are:

- sediment density,
- compressional-wave (or P-wave) speed,
- P-wave attenuation in decibels per wavelength,
- shear-wave (or S-wave) speed, and
- S-wave attenuation, also in decibels per wavelength.

The results of the modeling are supposed to represent the impact of the survey conducted inside the 3 nmi coastal zone. The most common sediment type for this zone is sand. For the purpose of acoustic propagation modeling the surficial sediment type was assumed to be “medium/fine sand” (grain size  $\phi = 2$ ) and porosity to be 50%. Generic geoacoustic properties for sand sediments were estimated using a sediment grain-shearing model (Buckingham 2005) that computes the acoustic properties of the sediments from porosity and grain-size. The bottom geoacoustic profile assumed for the sandy bottom is presented in Table 5.

Table 5. Geoacoustic properties of the sub-bottom sediments as a function of depth, in meters below the seafloor (mbsf) for sandy-bottom type. The properties for the sediment layers were derived from the assumed porosity and grain size according to the sediment grain-shearing model (Buckingham 2005).

Depth (mbsf)	Material	Density (g/cm <sup>3</sup> )	P-wave speed (m/s)	P-wave attenuation (dB/λ)	S-wave speed (m/s)	S-wave attenuation (dB/λ)
0–10	sand	1.87–1.87	1648–1785	0.45–0.9	300	0.1
10–50		1.87–2.0	1785–1987	0.9–1.45		

A map of benthic habitats shows the nearshore seabed has a significant amount of exposed bedrock (Endris and Greene 2011). In areas where the sea bottom is exposed bedrock, a hard-bottom geoacoustic profile was constructed. The geoacoustic properties were estimated based on the assumption of a highly weathered sandstone at the top 10 m and more typical values for the deeper layers (Table 6).

Table 6. Geoacoustic properties of the sub-bottom sediments as a function of depth, in meters below the seafloor (mbsf) for hard bottom type. Within each depth range, the parameters vary linearly within the stated range.

Depth (mbsf)	Material	Density (g/cm <sup>3</sup> )	P-wave speed (m/s)	P-wave attenuation (dB/λ)	S-wave speed (m/s)	S-wave attenuation (dB/λ)
0–10	Weathered	2.3–2.4	1850–2500	0.2–0.15	250	0.1
10–50	sandstone	2.4–2.6	2500–3000	0.15–0.1		
50–1000	Sandstone	2.6	3000–3500	0.1		
>1000			3500			

### 3.3.3. Sound Speed Profile

The sound speed profiles for the modeled site were obtained from the U.S. Naval Oceanographic Office's Generalized Digital Environmental Model (GDEM) database (Teague et al. 1990). The current release of the GDEM database (version 3.0) provides average monthly profiles of temperature and salinity for oceans on a latitude-longitude grid with  $0.25^\circ$  resolution, based on global historical observations from the U.S. Navy's Master Oceanographic Observation Data Set (MOODS). The profiles include 78 fixed depth points, up to a maximum depth of 6800 m (where the ocean is that deep), including 55 standard depths between 0 and 2000 m. The GDEM temperature-salinity profiles were converted to sound speed profiles according to the equations of Coppens (1981):

$$\begin{aligned}
 c(z, T, S, \phi) &= 1449.05 + 45.7t - 5.21t^2 - 0.23t^3 \\
 &\quad + (1.333 - 0.126t + 0.009t^2)(S - 35) + \Delta \\
 \Delta &= 16.3Z + 0.18Z^2 \\
 Z &= (z/1000)(1 - 0.0026\cos(2\phi)) \\
 t &= T/10
 \end{aligned} \tag{10}$$

where  $z$  is water depth (m),  $T$  is water temperature ( $^\circ\text{C}$ ),  $S$  is salinity (psu), and  $\phi$  is latitude (radians).

At the time of this report, it was unknown in which months the geophysical surveys will take place. The analysis of the sound speed profile evolution through one complete year was performed. The most distinct months, February, March, April, July, and September, are plotted in Figure 13. All profiles present downward refracting characteristics in the top 100 m of water (negative gradient of the sound speed with depth). A down refracting sound speed profile directs the acoustic wave downward, leading to greater interaction with the bottom and, consequently, greater attenuation with distance compared to other types of sound speed profiles. The down refracting characteristic is less pronounced on the sound speed profile for February, which promotes longer sound propagation. This precautionary profile (leading to larger distances to threshold levels) was used in this modeling study.

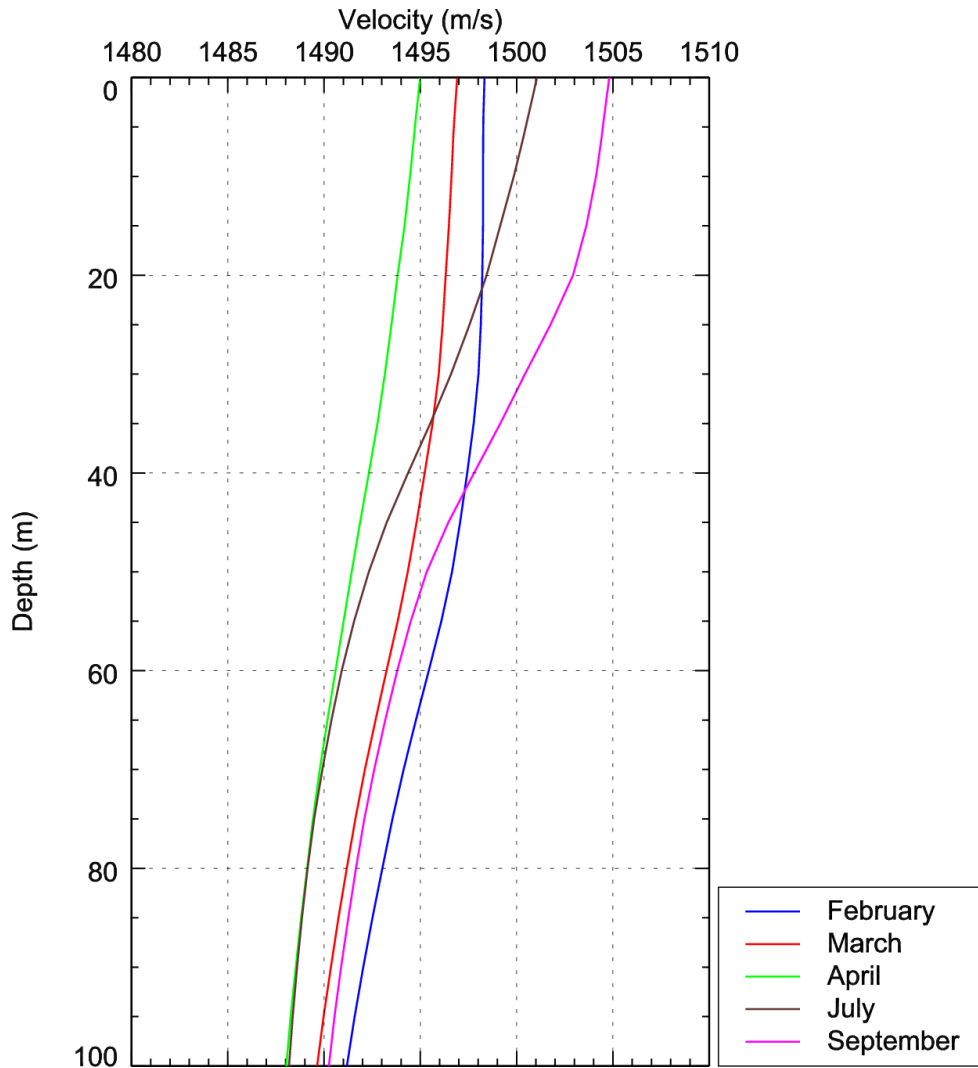


Figure 13. Sound speed profiles derived from historical monthly average water temperature and salinity (GDEM database) for February, March, April, July, and September.

---

## Results

---

### 4.1. Per-pulse Threshold Distances

The per-pulse threshold radii for the five instruments under investigation are presented in Table 7 through Table 16. The maps of maximum-over-depth sound pressure levels around the sources are provided for the scenarios with sand-bottom environments only (Figure 14 through Figure 18).

For each sound level threshold, two statistical estimates of the safety radii are provided: (1) the maximum range ( $R_{\max}$ , in meters) and (2) the 95% range ( $R_{95\%}$ , in meters). Given a regularly gridded spatial distribution of sound levels, the  $R_{95\%}$  for a given sound level is defined as the radius of the circle, centered on the source, encompassing 95% of the grid points with sound levels at or above the given value. This definition is meaningful in terms of potential impact to animals because, regardless of the shape of the contour for a given sound level,  $R_{95\%}$  is the range from the source beyond which less than 5% of a uniformly distributed population would be exposed to sound at or above that level. The  $R_{\max}$  for a given sound level is simply the distance to the farthest occurrence of the threshold level (equivalent to  $R_{100\%}$ ). It is more conservative than  $R_{95\%}$  but may overestimate the effective exposure zone. For cases where the volume ensonified to a specific level is discontinuous and small pockets of higher received levels occur far beyond the main ensonified volume (e.g., due to convergence),  $R_{\max}$  would be much larger than  $R_{95\%}$  and could therefore be misleading if not given along with  $R_{95\%}$ .

Table 7. *Single beam echosounder Odom CV-100 (sandy bottom)*: Maximum ( $R_{max}$ , m) and 95% ( $R_{95\%}$ , m) horizontal distances from the source to modeled maximum-over-depth sound level thresholds, with and without M-weighting applied for low-frequency cetaceans (LFC), mid-frequency cetaceans (MFC), high-frequency cetaceans (HFC), and pinnipeds.

	Un-weighted		LFC		MFC		HFC		Pinnipeds	
	$R_{max}$	$R_{95\%}$	$R_{max}$	$R_{95\%}$	$R_{max}$	$R_{95\%}$	$R_{max}$	$R_{95\%}$	$R_{max}$	$R_{95\%}$
<i>rms SPL (dB re 1 <math>\mu</math>Pa)</i>										
208	-	-	-	-	-	-	-	-	-	-
206	-	-	-	-	-	-	-	-	-	-
190	-	-	-	-	-	-	-	-	-	-
180	<20	<20	-	-	-	-	-	-	-	-
160	25	25			<20	<20	<20	<20	<20	<20
140	101	98	<20	<20	60	57	63	61	28	27
120	347	326	28	27	229	206	248	224	116	106
<i>SEL (dB re 1 <math>\mu</math>Pa<sup>2</sup>·s)</i>										
198	-	-	-	-	-	-	-	-	-	-
192	-	-	-	-	-	-	-	-	-	-
187	<20	<20	<20	<20	<20	<20	<20	<20	<20	<20
186	<20	<20	<20	<20	<20	<20	<20	<20	<20	<20
183	<20	<20	<20	<20	<20	<20	<20	<20	<20	<20
179	<20	<20	<20	<20	<20	<20	<20	<20	<20	<20
171	<20	<20	<20	<20	<20	<20	<20	<20	<20	<20

Table 8. *Multibeam echosounder R2Sonic 2022 (sandy bottom)*: Maximum ( $R_{max}$ , m) and 95% ( $R_{95\%}$ , m) horizontal distances from the source to modeled maximum-over-depth sound level thresholds, with and without M-weighting applied for low-frequency cetaceans (LFC), mid-frequency cetaceans (MFC), high-frequency cetaceans (HFC), and pinnipeds.

	Un-weighted		LFC		MFC		HFC		Pinnipeds	
	$R_{max}$	$R_{95\%}$	$R_{max}$	$R_{95\%}$	$R_{max}$	$R_{95\%}$	$R_{max}$	$R_{95\%}$	$R_{max}$	$R_{95\%}$
<i>rms SPL (dB re 1 <math>\mu</math>Pa)</i>										
208	<20	<20	-	-	<20	<20	<20	<20	-	-
206	<20	<20	-	-	<20	<20	<20	<20	-	-
190	28	28	-	-	<20	<20	<20	<20	<20	<20
180	71	71	<20	<20	35	35	35	35	<20	<20
160	290	258	<20	<20	205	184	219	191	85	85
140	612	477	85	85	467	396	495	403	332	283
120	933	612	318	279	778	548	803	559	626	492
<i>SEL (dB re 1 <math>\mu</math>Pa<sup>2</sup>·s)</i>										
198	-	-	-	-	-	-	-	-	-	-
192	-	-	-	-	-	-	-	-	-	-
187	<20	<20	<20	<20	<20	<20	<20	<20	<20	<20
186	<20	<20	<20	<20	<20	<20	<20	<20	<20	<20
183	<20	<20	<20	<20	<20	<20	<20	<20	<20	<20
179	<20	<20	<20	<20	<20	<20	<20	<20	<20	<20
171	<20	<20	<20	<20	<20	<20	<20	<20	<20	<20

Table 9. Side-scan sonar Klein 3000 (sandy bottom): Maximum ( $R_{\max}$ , m) and 95% ( $R_{95\%}$ , m) horizontal distances from the source to modeled maximum-over-depth sound level thresholds, with and without M-weighting applied for low-frequency cetaceans (LFC), mid-frequency cetaceans (MFC), high-frequency cetaceans (HFC), and pinnipeds.

	Un-weighted		LFC		MFC		HFC		Pinnipeds	
	$R_{\max}$	$R_{95\%}$	$R_{\max}$	$R_{95\%}$	$R_{\max}$	$R_{95\%}$	$R_{\max}$	$R_{95\%}$	$R_{\max}$	$R_{95\%}$
<i>rms SPL (dB re 1 <math>\mu</math>Pa)</i>										
208	<20	<20	-	-	<20	<20	<20	<20	<20	<20
206	<20	<20	-	-	<20	<20	<20	<20	<20	<20
190	130	124	<20	<20	73	68	96	88	31	31
180	257	243	<20	<20	187	181	209	195	102	96
160	682	576	110	102	611	512	625	526	441	399
140	1,106	690	455	413	1,007	689	1021	696	837	675
120	1,544	917	880	683	1,445	860	1445	867	1,261	795
<i>SEL (dB re 1 <math>\mu</math>Pa<sup>2</sup>·s)</i>										
198	<20	<20	-	-	-	-	-	-	-	-
192	<20	<20	-	-	<20	<20	<20	<20	-	-
187	<20	<20	-	-	<20	<20	<20	<20	<20	<20
186	<20	<20	-	-	<20	<20	<20	<20	<20	<20
183	<20	<20	-	-	<20	<20	<20	<20	<20	<20
179	<20	<20	-	-	<20	<20	<20	<20	<20	<20
171	31	31	-	-	<20	<20	<20	<20	<20	<20

Table 10. Side-scan sonar Klein 3000 (exposed bedrock bottom): Maximum ( $R_{\max}$ , m) and 95% ( $R_{95\%}$ , m) horizontal distances from the source to modeled maximum-over-depth sound level thresholds, with and without M-weighting applied for low-frequency cetaceans (LFC), mid-frequency cetaceans (MFC), high-frequency cetaceans (HFC), and pinnipeds.

	Un-weighted		LFC		MFC		HFC		Pinnipeds	
	$R_{\max}$	$R_{95\%}$	$R_{\max}$	$R_{95\%}$	$R_{\max}$	$R_{95\%}$	$R_{\max}$	$R_{95\%}$	$R_{\max}$	$R_{95\%}$
<i>rms SPL (dB re 1 <math>\mu</math>Pa)</i>										
208	<20	<20	-	-	<20	<20	<20	<20	<20	<20
206	<20	<20	-	-	<20	<20	<20	<20	<20	<20
190	130	124	<20	<20	85	85	96	88	42	42
180	269	255	<20	<20	187	181	212	212	102	99
160	693	587	113	113	622	523	625	526	453	410
140	1,131	721	467	424	1,047	700	1,061	700	877	686
120	1,584	935	880	686	1,485	873	1,499	880	1,329	795
<i>SEL (dB re 1 <math>\mu</math>Pa<sup>2</sup>·s)</i>										
198	<20	<20	-	-	-	-	-	-	-	-
192	<20	<20	-	-	<20	<20	<20	<20	-	-
187	<20	<20	-	-	<20	<20	<20	<20	<20	<20
186	<20	<20	-	-	<20	<20	<20	<20	<20	<20
183	<20	<20	-	-	<20	<20	<20	<20	<20	<20
179	<20	<20	-	-	<20	<20	<20	<20	<20	<20
171	31	31	-	-	<20	<20	<20	<20	<20	<20

Table 11. *Sub-bottom profiler EdgeTech X-Star (sandy bottom):* Maximum ( $R_{max}$ , m) and 95% ( $R_{95\%}$ , m) horizontal distances from the source to modeled maximum-over-depth sound level thresholds, with and without M-weighting applied for low-frequency cetaceans (LFC), mid-frequency cetaceans (MFC), high-frequency cetaceans (HFC), and pinnipeds.

	Un-weighted		LFC		MFC		HFC		Pinnipeds	
	$R_{max}$	$R_{95\%}$	$R_{max}$	$R_{95\%}$	$R_{max}$	$R_{95\%}$	$R_{max}$	$R_{95\%}$	$R_{max}$	$R_{95\%}$
<i>rms SPL (dB re 1 <math>\mu</math>Pa)</i>										
208	-	-	-	-	-	-	-	-	-	-
206	-	-	-	-	-	-	-	-	-	-
190	<20	<20	<20	<20	<20	<20	<20	<20	<20	<20
180	<20	<20	<20	<20	<20	<20	<20	<20	<20	<20
160	36	36	32	32	36	36	36	36	36	36
140	607	292	240	225	607	291	607	291	602	283
120	6,699	5,439	6,151	4,888	6,699	5,424	6,699	5,426	6,689	5,383
<i>SEL (dB re 1 <math>\mu</math>Pa<sup>2</sup>·s)</i>										
198	-	-	-	-	-	-	-	-	-	-
192	-	-	-	-	-	-	-	-	-	-
187	<20	<20	<20	<20	<20	<20	<20	<20	<20	<20
186	<20	<20	<20	<20	<20	<20	<20	<20	<20	<20
183	<20	<20	<20	<20	<20	<20	<20	<20	<20	<20
179	<20	<20	<20	<20	<20	<20	<20	<20	<20	<20
171	<20	<20	<20	<20	<20	<20	<20	<20	<20	<20

Table 12. *Boomer AP3000 triple-plate configuration (sandy bottom):* Maximum ( $R_{max}$ , m) and 95% ( $R_{95\%}$ , m) horizontal distances from the source to modeled maximum-over-depth sound level thresholds, with and without M-weighting applied for low-frequency cetaceans (LFC), mid-frequency cetaceans (MFC), high-frequency cetaceans (HFC), and pinnipeds.

	Un-weighted		LFC		MFC		HFC		Pinnipeds	
	$R_{max}$	$R_{95\%}$	$R_{max}$	$R_{95\%}$	$R_{max}$	$R_{95\%}$	$R_{max}$	$R_{95\%}$	$R_{max}$	$R_{95\%}$
<i>rms SPL (dB re 1 <math>\mu</math>Pa)</i>										
208	-	-	-	-	-	-	-	-	-	-
206	-	-	-	-	-	-	-	-	-	-
190	<20	<20	<20	<20	<20	<20	<20	<20	<20	<20
180	<20	<20	<20	<20	<20	<20	<20	<20	<20	<20
160	50	45	45	45	45	45	45	45	45	45
140	2,329	1,567	2,329	1,563	2,228	1,462	2,224	1,393	2,329	1,538
120	28,110	19,229	28,110	19,184	27,820	18,446	27,818	17,909	28,110	18,968
<i>SEL (dB re 1 <math>\mu</math>Pa<sup>2</sup>·s)</i>										
198	-	-	-	-	-	-	-	-	-	-
192	-	-	-	-	-	-	-	-	-	-
187	-	-	-	-	-	-	-	-	-	-
186	-	-	-	-	-	-	-	-	-	-
183	<20	<20	<20	<20	<20	<20	<20	<20	<20	<20
179	<20	<20	<20	<20	<20	<20	<20	<20	<20	<20
171	<20	<20	<20	<20	<20	<20	<20	<20	<20	<20

Table 13. *Boomer AP3000 triple-plate system (exposed bedrock bottom)*: Maximum ( $R_{max}$ , m) and 95% ( $R_{95\%}$ , m) horizontal distances from the source to modeled maximum-over-depth sound level thresholds, with and without M-weighting applied for low-frequency cetaceans (LFC), mid-frequency cetaceans (MFC), high-frequency cetaceans (HFC), and pinnipeds.

	Un-weighted		LFC		MFC		HFC		Pinnipeds	
	$R_{max}$	$R_{95\%}$	$R_{max}$	$R_{95\%}$	$R_{max}$	$R_{95\%}$	$R_{max}$	$R_{95\%}$	$R_{max}$	$R_{95\%}$
<i>rms SPL (dB re 1 <math>\mu</math>Pa)</i>										
208	-	-	-	-	-	-	-	-	-	-
206	-	-	-	-	-	-	-	-	-	-
190	<20	<20	<20	<20	<20	<20	<20	<20	<20	<20
180	<20	<20	<20	<20	<20	<20	<20	<20	<20	<20
160	89	89	89	89	57	57	45	45	89	89
140	4,871	3,005	4,871	3,000	4,262	2,773	4,197	2,635	4,328	2,930
120	61,919	43,202	61,666	43,156	61,663	41,142	59,765	39,835	61,663	42,619
<i>SEL (dB re 1 <math>\mu</math>Pa<sup>2</sup>·s)</i>										
198	-	-	-	-	-	-	-	-	-	-
192	-	-	-	-	-	-	-	-	-	-
187	-	-	-	-	-	-	-	-	-	-
186	-	-	-	-	-	-	-	-	-	-
183	<20	<20	<20	<20	<20	<20	<20	<20	<20	<20
179	<20	<20	<20	<20	<20	<20	<20	<20	<20	<20
171	<20	<20	<20	<20	<20	<20	<20	<20	<20	<20

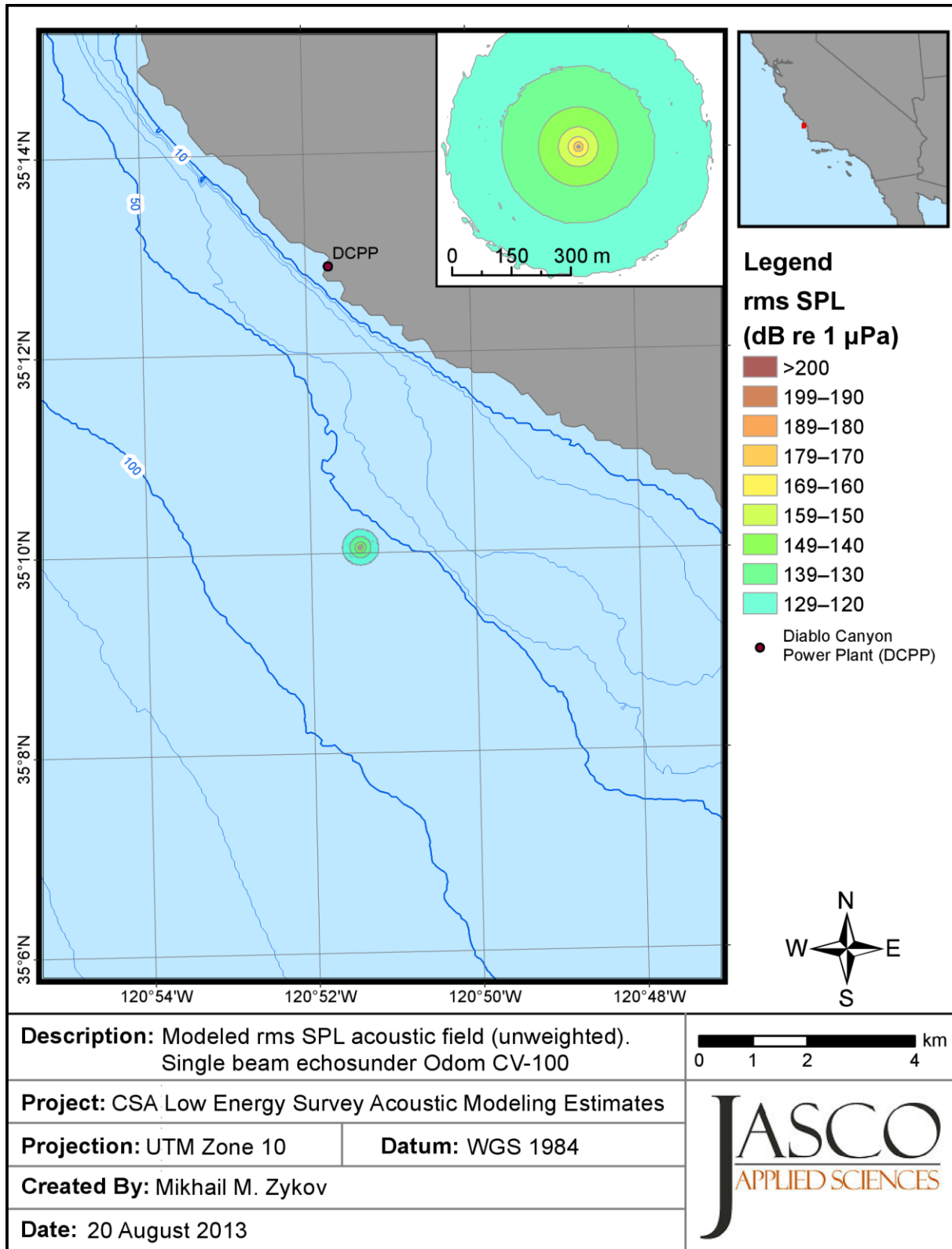


Figure 14. Odom CV-100 single beam echosounder. Maximum-over-depth (200 kHz) sound pressure levels around the source. Bathymetry contours (m) are shown in blue.

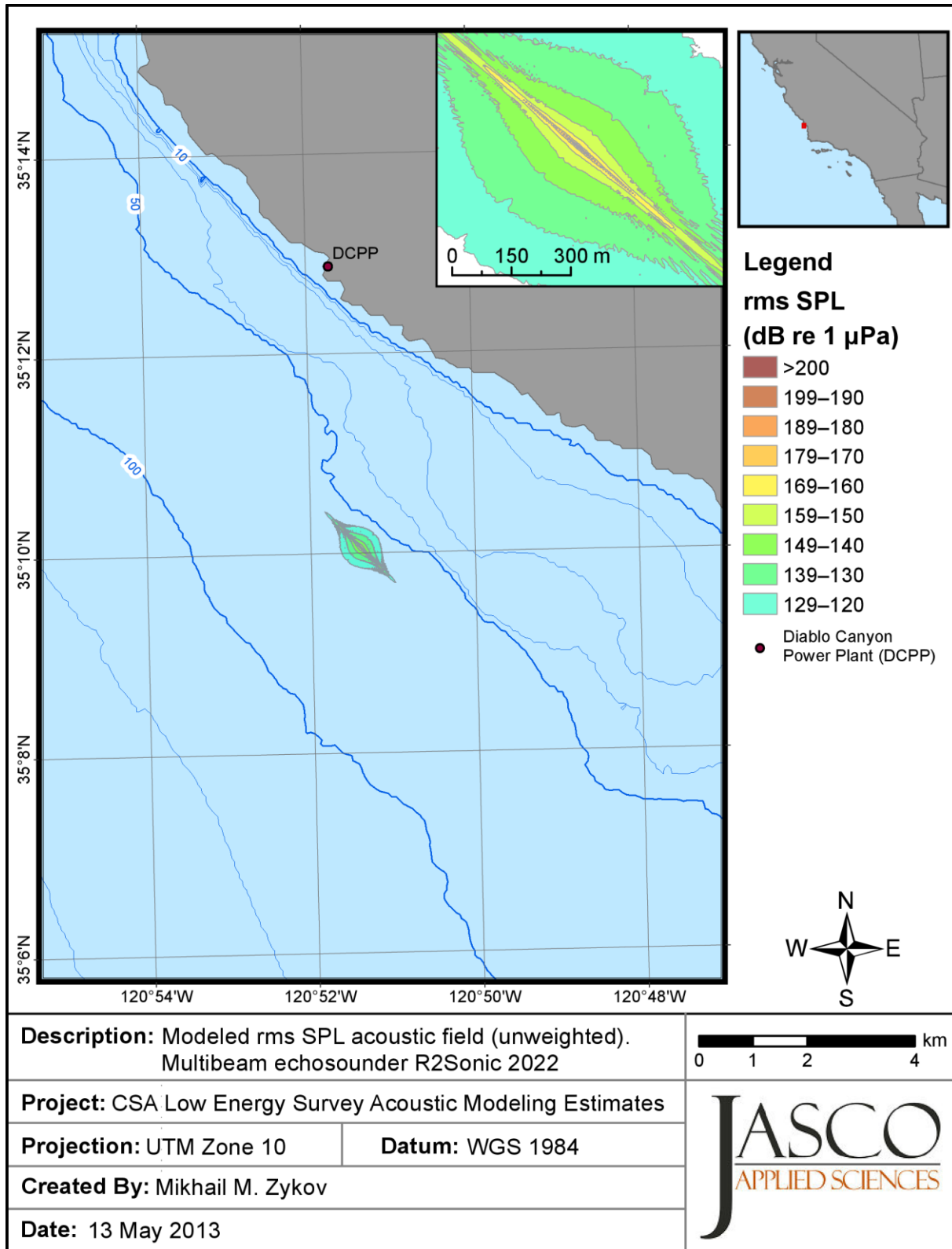


Figure 15. R2Sonic 2022 multibeam echosounder. Maximum-over-depth (200 kHz) sound pressure levels around the source. Bathymetry contours (m) are shown in blue.

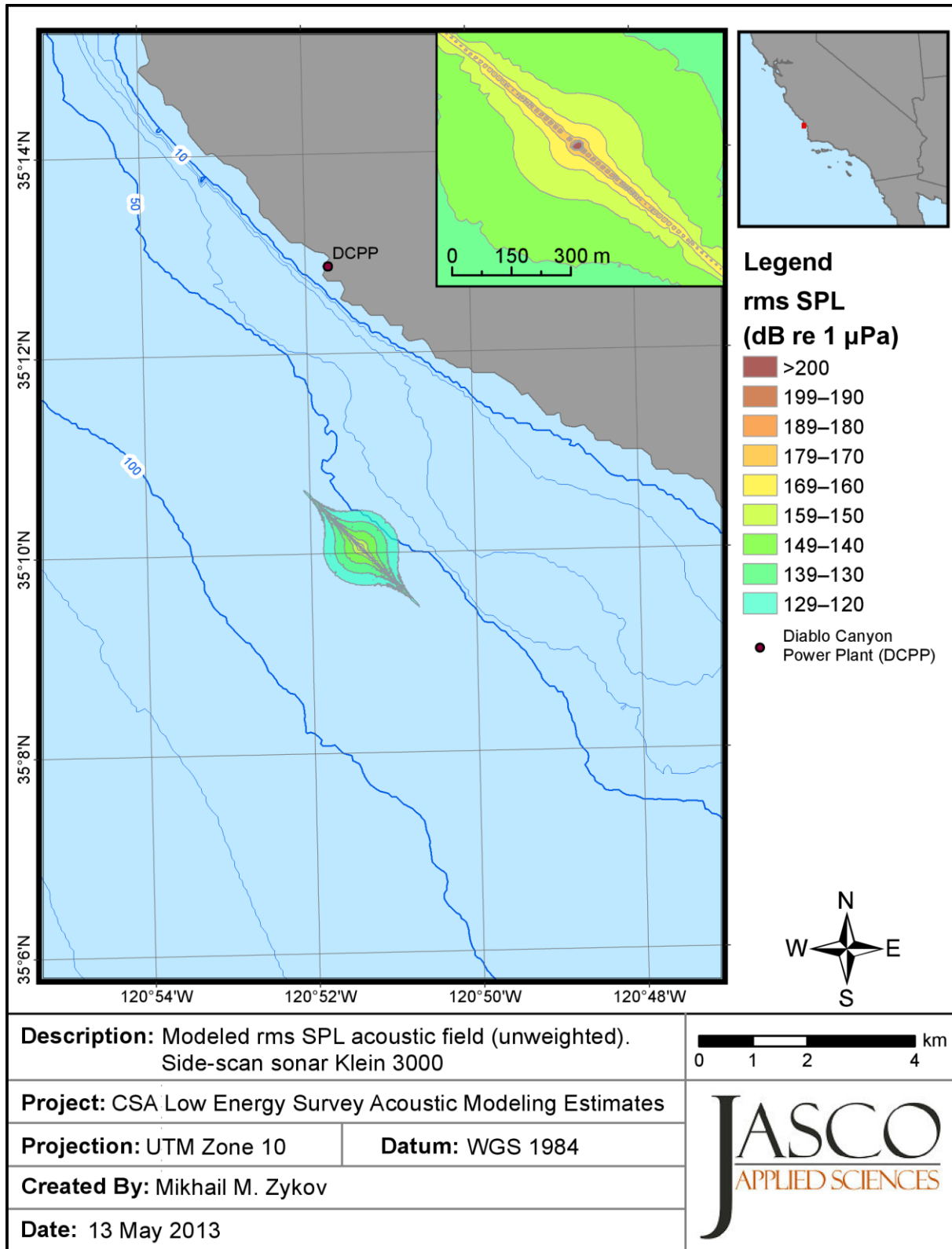


Figure 16. Klein 3000 side-scan sonar. Maximum-over-depth (132 kHz) sound pressure levels around the source. Bathymetry contours (m) are shown in blue.

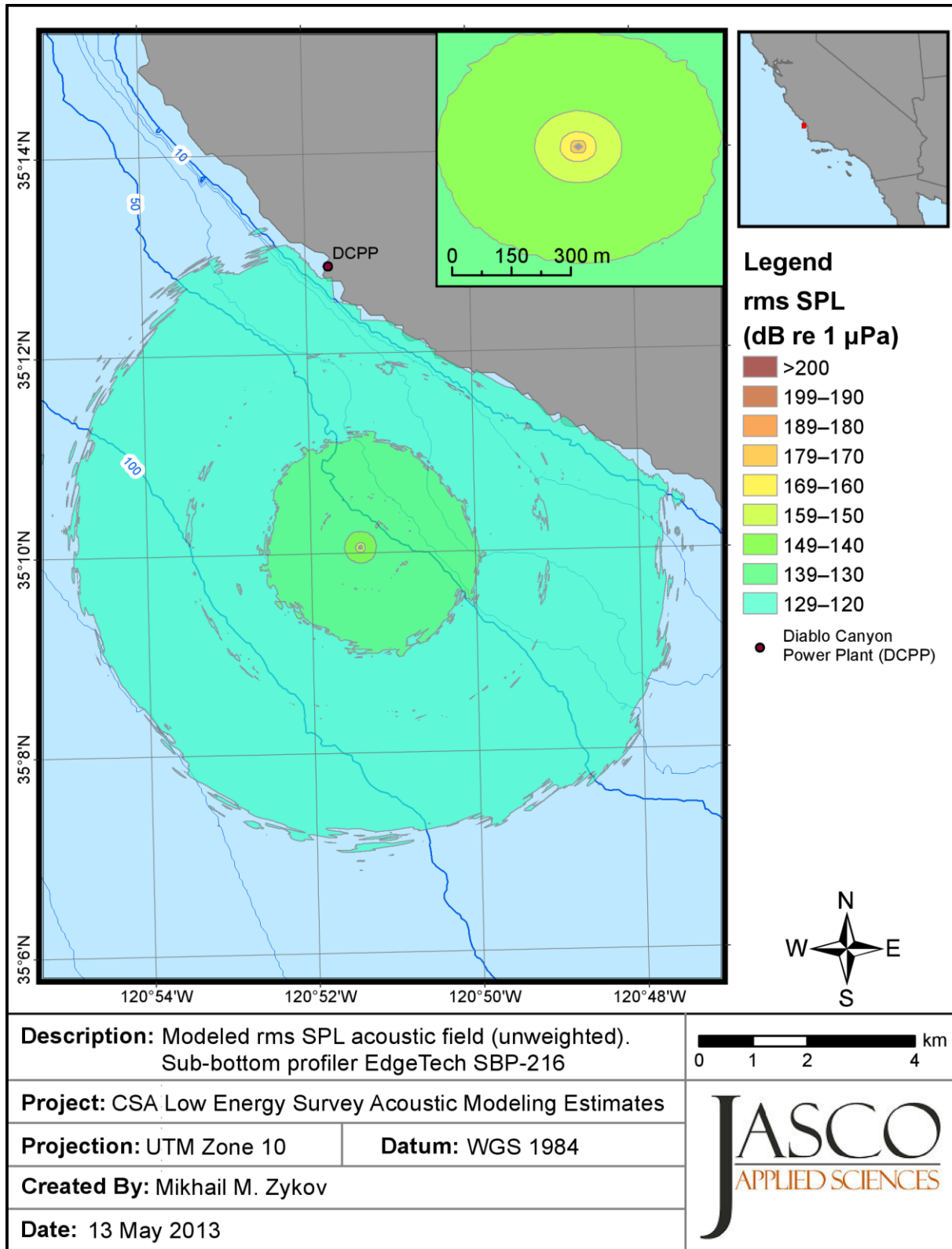


Figure 17. EdgeTech SBP-216 sub-bottom profiler. Maximum-over-depth (9 kHz) sound pressure levels around the source. Bathymetry contours (m) are shown in blue.

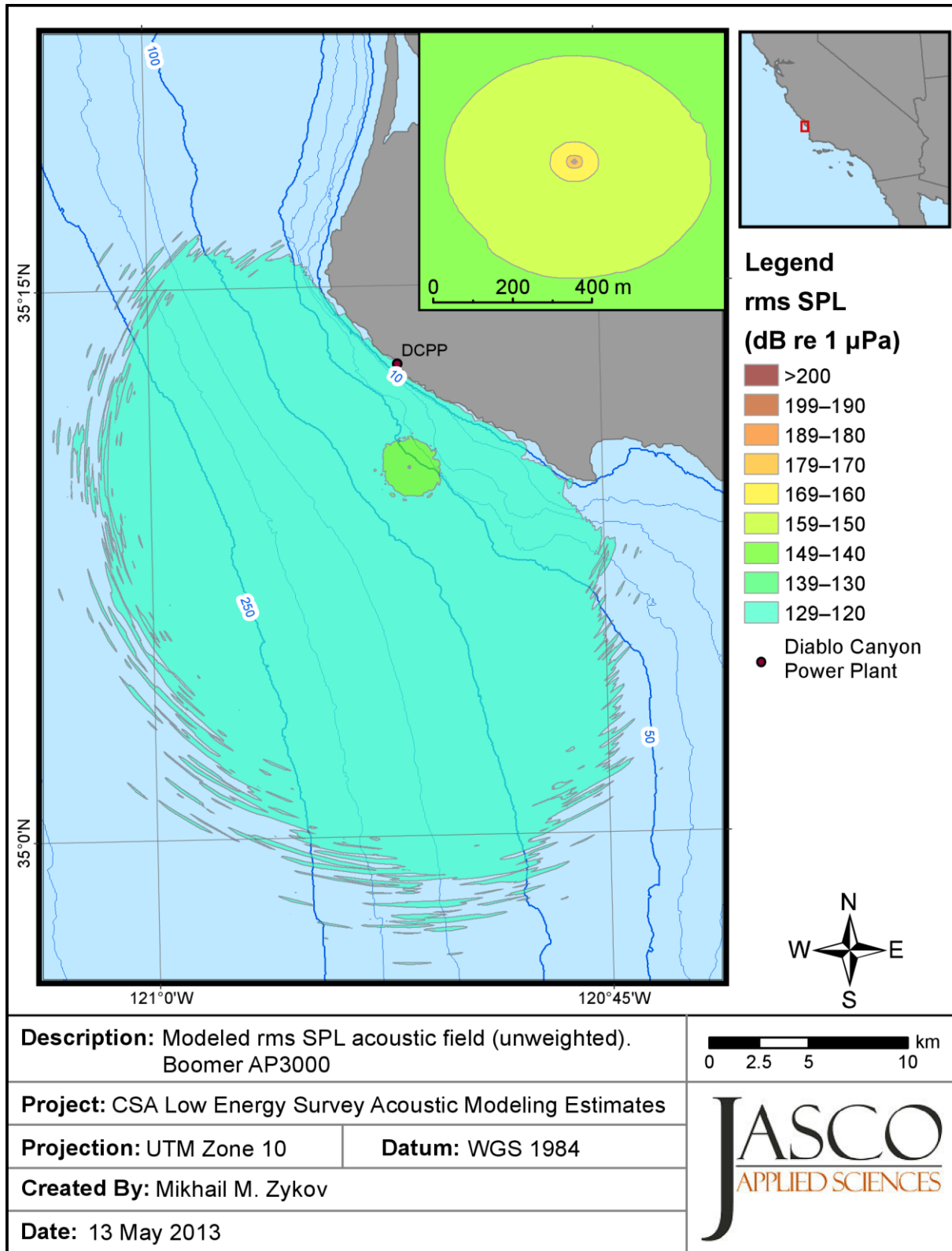


Figure 18. AP3000 boomer in triple plate configuration: Maximum-over-depth broadband (200–16000 Hz) sound pressure levels around the source. Bathymetry contours (m) are shown in blue.

## 4.2. Cumulative Field

The area affected by the specific threshold cumulative sound exposure level (cSEL) for three line scenarios with multibeam echosounder, side-scan sonar, and sub-bottom profiler are presented in Table 14, Table 15, and Table 16, respectively. Approximate radii from the source to the specific threshold cSEL are also indicated. The same data are provided for the complex scenario in Table 17. The source levels for the single beam echosounder and boomer, in terms of SEL, were not high enough to produce cSEL above the minimum threshold of interest at distances from the source that are significant enough to consider. The map of the cSEL acoustic field for the complex scenario is shown in Figure 19.

Table 14. *Multibeam echosounder R2Sonic 2022*: Affected area by specific cumulative sound exposure level (cSEL) thresholds and the approximate distance from the source to modeled maximum-over-depth cumulative thresholds, with and without M-weighting applied for low-frequency cetaceans (LFC), mid-frequency cetaceans (MFC), high-frequency cetaceans (HFC), and pinnipeds.

	Un-weighted		LFC		MFC		HFC		Pinnipeds	
	Area (km <sup>2</sup> )	Radius (m)								
<i>SEL (dB re 1 <math>\mu</math>Pa<sup>2</sup>·s)</i>										
198	-	-	-	-	-	-	-	-	-	-
192	-	-	-	-	-	-	-	-	-	-
186	-	-	-	-	-	-	-	-	-	-
183	0.008	1.0	-	-	-	-	-	-	-	-
179	0.011	1.5	-	-	-	-	0.002	0.5	-	-
171	0.020	2.0	-	-	0.011	1.5	0.013	1.5	-	-

Table 15. *Side-scan sonar Klein 3000*: Affected area by specific cumulative sound exposure level (cSEL) thresholds and the approximate distance from the source to modeled maximum-over-depth cumulative thresholds, with and without M-weighting applied for low-frequency cetaceans (LFC), mid-frequency cetaceans (MFC), high-frequency cetaceans (HFC), and pinnipeds.

	Un-weighted		LFC		MFC		HFC		Pinnipeds	
	Area (km <sup>2</sup> )	Radius (m)								
<i>SEL (dB re 1 <math>\mu</math>Pa<sup>2</sup>·s)</i>										
198	-	-	-	-	-	-	-	-	-	-
192	-	-	-	-	-	-	-	-	-	-
186	0.009	1.0	-	-	-	-	-	-	-	-
183	0.011	1.5	-	-	0.009	1.0	0.009	1.0	-	-
179	0.015	1.5	-	-	0.011	1.5	0.011	1.5	-	-
171	0.04	3	-	-	0.02	2.0	0.02	2.0	0.01	1.5

Table 16. *Sub-bottom profiler EdgeTech X-Star*: Affected area by specific cumulative sound exposure level (cSEL) thresholds and the approximate distance from the source to modeled maximum-over-depth cumulative thresholds, with and without M-weighting applied for low-frequency cetaceans (LFC), mid-frequency cetaceans (MFC), high-frequency cetaceans (HFC), and pinnipeds.

	Un-weighted		LFC		MFC		HFC		Pinnipeds	
	Area (km <sup>2</sup> )	Radius (m)								
<i>SEL (dB re 1 μPa<sup>2</sup>·s)</i>										
198	-	-	-	-	-	-	-	-	-	-
192	-	-	-	-	-	-	-	-	-	-
186	0.01	1.5	0.01	1.5	0.01	1.5	0.01	1.5	0.01	1.5
183	0.02	2.0	0.02	2.0	0.02	2.0	0.02	2.0	0.02	2.0
179	0.03	2.5	0.03	2.5	0.03	2.5	0.03	2.5	0.03	2.5
171	0.05	3.0	0.05	3.0	0.05	3.0	0.05	3.0	0.05	3.0

Table 17. *Complex scenario*: Affected area by specific cumulative sound exposure level (cSEL) thresholds and the approximate distance from the source to modeled maximum-over-depth cumulative thresholds, with and without M-weighting applied for low-frequency cetaceans (LFC), mid-frequency cetaceans (MFC), high-frequency cetaceans (HFC), and pinnipeds.

	Un-weighted		LFC		MFC		HFC		Pinnipeds	
	Area (km <sup>2</sup> )	Radius (m)								
<i>SEL (dB re 1 μPa<sup>2</sup>·s)</i>										
198	0.008	1.0	-	-	0.001	0.5	0.001	0.5	-	-
192	0.013	1.5	0.001	0.5	0.010	1.0	0.011	1.0	0.004	0.5
186	0.017	1.5	0.011	1.0	0.015	1.5	0.015	1.5	0.013	1.5
183	0.020	2.0	0.014	1.5	0.018	2.0	0.018	2.0	0.016	1.5
179	0.027	2.5	0.018	2.0	0.022	2.0	0.022	2.0	0.020	2.0
171	0.143	35	0.043	3.5	0.072	15	0.080	18	0.060	8

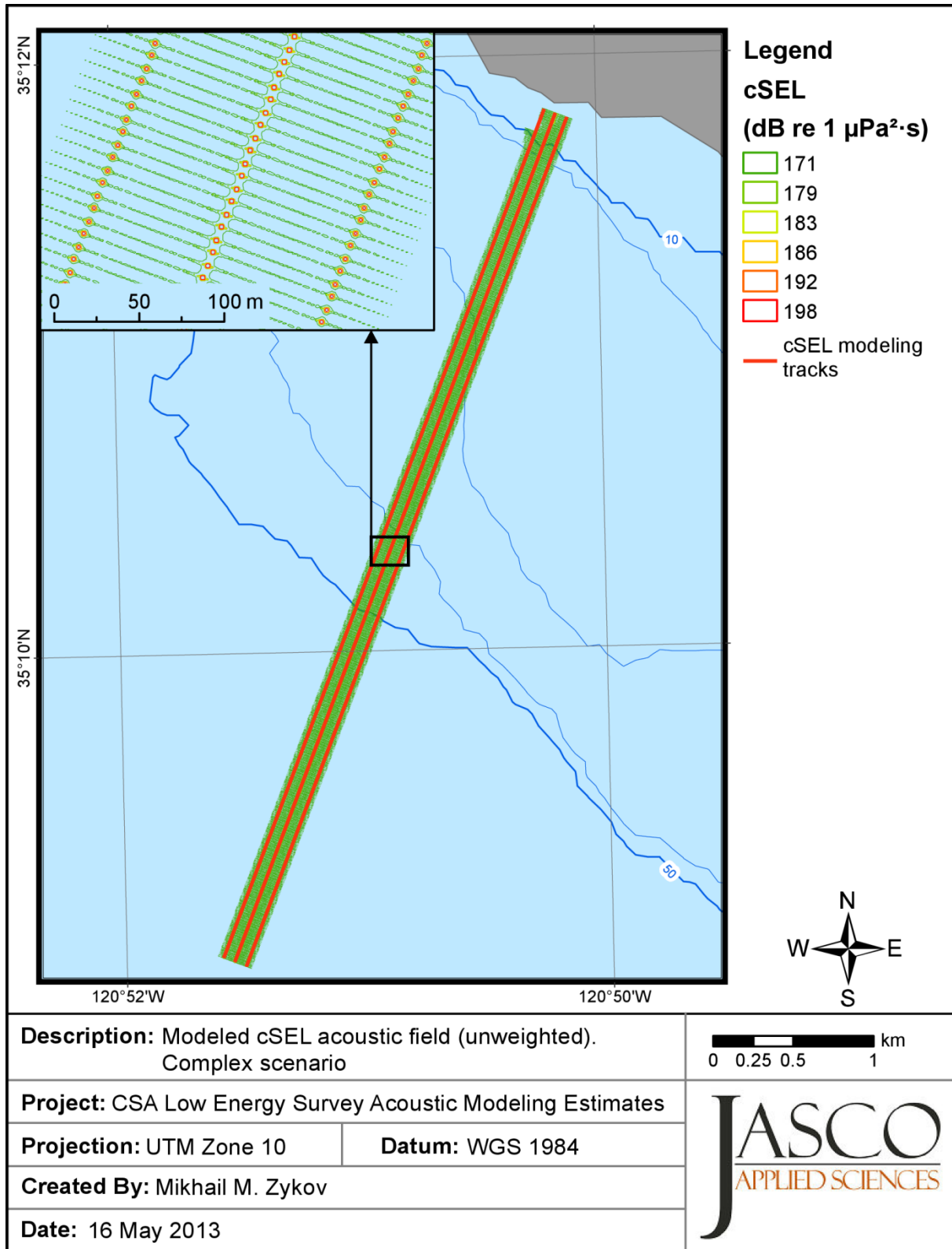


Figure 19. Complex scenario for the cumulative sound exposure level (cSEL) acoustic field. Bathymetry contours (m) are shown in blue.

***Effect of Altered Pulse Rate on Cumulative Field Sound Exposure Calculations***

During review of the draft MND, a question was raised as to the potential effects of a change in pulse rate on cumulative SEL levels. The pulse rate chosen for modeling was based on coordination with geophysical industry contacts, and is considered to be representative of OGPP survey activities. The pulse rate is highly variable parameter of the survey that depends on environmental factors as well as on the purpose of the survey. For example, if the modeled pulse rate of 1 pulse per 4 seconds is changed to 2 pulses per second or 4 pulses per second, reviewers were interested in determining what effects such a change would have on cSEL. While conducting additional modeling to address this question was not feasible during MND finalization, JASCO was able to approximate the cSEL calculations, as detailed below.

The increase in the cSEL with increasing pulse rate would be  $10 \cdot \text{LOG}_{10}(N)$  where N is the multiplication of the rate. If the rate of 1 pulse per 4 seconds is increased to 2 pulses per 1 second ( $N=8$ ) or 4 pulses per 1 second ( $N=16$ ), the increase in cSEL would be 9 and 12 dB, respectively. Such changes in pulse rate would shift values by the corresponding dB. For  $N=8$ , the addition of 9 dB would place cSEL in a position approximately where 171 dB was previously located. For +12 dB, the 181 dB will move to 171 dB.

Approximate cumulative exposure calculations for the multibeam echosounder, side scan sonar, and subbottom profiler, at pulse rates of 2 and 4 pulses per second, are provided in Tables 18 through 23.

Table 18. Approximate cumulative sound exposure levels for multibeam echosounder, with unweighted and M-weighted radial distances and area ensonified at a pulse rate of 2 pulses per second.

cSEL (dB re 1 $\mu\text{Pa}^2\cdot\text{s}$ )		No Weighting		M-Weighted							
				LF Cetaceans		MF Cetaceans		HF Cetaceans		Pinnipeds	
		Area ( $\text{km}^2$ )	Radius (m)								
Injury	198	-	-	-	-	-	-	-	-	-	-
	192	~0.008	~1.0	-	-	-	-	-	-	-	-
	186	>0.011	>1.5	-	-	-	-	>0.002	>0.5		
	179	>0.020	>2.0	-	-	0.011	1.5	>0.013	>1.5	-	-
Behavioral Modification	183	<0.020	<2.0	-	-	<0.011	<1.5	<0.013	<1.5	-	-
	171	N/A	N/A								

Injury: 198 dB re 1  $\mu\text{Pa}^2\cdot\text{s}$  = mid-frequency (MF) cetaceans; 192 dB re 1  $\mu\text{Pa}^2\cdot\text{s}$  = low-frequency (LF) cetaceans; 186 dB re 1  $\mu\text{Pa}^2\cdot\text{s}$  = pinnipeds (in water); 179 dB re 1  $\mu\text{Pa}^2\cdot\text{s}$  = high-frequency (HF) cetaceans.

Behavioral Modification: 183 dB re 1  $\mu\text{Pa}^2\cdot\text{s}$  = low- (LF), mid- (MF), and high-frequency (HF) cetaceans; 171 dB re 1  $\mu\text{Pa}^2\cdot\text{s}$  = pinnipeds (in water).

Dark gray shading indicates entries which are not applicable to the respective SEL threshold/M-weighting classification.

N/A – not available; requires recalculation.

Table 19. Approximate cumulative sound exposure levels for multibeam echosounder, with unweighted and M-weighted radial distances and area ensonified at a pulse rate of 4 pulses per second.

cSEL (dB re 1 $\mu\text{Pa}^2\cdot\text{s}$ )		No Weighting		M-Weighted							
				LF Cetaceans		MF Cetaceans		HF Cetaceans		Pinnipeds	
		Area (km <sup>2</sup> )	Radius (m)								
Injury	198	-	-	-	-	-	-	-	-	-	-
	192	~0.011	~1.5	-	-	-	-	~0.002	~0.5	-	-
	186	<0.020	<2.0	-	-	<0.011	<1.5	<0.013	<1.5	-	-
	179	N/A	N/A								
Behavioral Modification	183	~0.020	~2.0	-	-	~0.011	~1.5	~0.013	~1.5	-	-
	171	N/A	N/A								

Injury: 198 dB re 1  $\mu\text{Pa}^2\cdot\text{s}$  = mid-frequency (MF) cetaceans; 192 dB re 1  $\mu\text{Pa}^2\cdot\text{s}$  = low-frequency (LF) cetaceans; 186 dB re 1  $\mu\text{Pa}^2\cdot\text{s}$  = pinnipeds (in water); 179 dB re 1  $\mu\text{Pa}^2\cdot\text{s}$  = high-frequency (HF) cetaceans.

Behavioral Modification: 183 dB re 1  $\mu\text{Pa}^2\cdot\text{s}$  = low- (LF), mid- (MF), and high-frequency (HF) cetaceans; 171 dB re 1  $\mu\text{Pa}^2\cdot\text{s}$  = pinnipeds (in water).

Dark gray shading indicates entries which are not applicable to the respective SEL threshold/M-weighting classification.

N/A – not available; requires recalculation.

Table 20. Approximate cumulative sound exposure levels for side-scan sonar, with unweighted and M-weighted radial distances and area ensonified at a pulse rate of 2 pulses per second.

cSEL (dB re 1 $\mu\text{Pa}^2\cdot\text{s}$ )		No Weighting		M-Weighted							
				LF Cetaceans		MF Cetaceans		HF Cetaceans		Pinnipeds	
		Area ( $\text{km}^2$ )	Radius (m)								
Injury	198	<0.009	<1.0	-	-	-	-	-	-	-	-
	192	~0.011	~1.5	-	-	~0.009	~1.0	~0.009	~1.0	-	-
	186	>0.015	>1.5	-	-	>0.011	>1.5	>0.011	>1.5	-	-
	179	>0.04	>3.0	-	-	>0.02	>2.0	>0.02	>2.0	>0.01	>1.5
Behavioral Modification	183	<0.04	<3.0	-	-	<0.02	<2.0	<0.02	<2.0	<0.01	<1.5
	171	N/A	N/A								

Injury: 198 dB re 1  $\mu\text{Pa}^2\cdot\text{s}$  = mid-frequency (MF) cetaceans; 192 dB re 1  $\mu\text{Pa}^2\cdot\text{s}$  = low-frequency (LF) cetaceans; 186 dB re 1  $\mu\text{Pa}^2\cdot\text{s}$  = pinnipeds (in water); 179 dB re 1  $\mu\text{Pa}^2\cdot\text{s}$  = high-frequency (HF) cetacean.

Behavioral Modification: 183 dB re 1  $\mu\text{Pa}^2\cdot\text{s}$  = low- (LF), mid- (MF), and high-frequency (HF) cetaceans; 171 dB re 1  $\mu\text{Pa}^2\cdot\text{s}$  = pinnipeds (in water).

Dark gray shading indicates entries which are not applicable to the respective SEL threshold/M-weighting classification.

N/A – not available; requires recalculation.

Table 21. Approximate cumulative sound exposure levels for side-scan sonar, with unweighted and M-weighted radial distances and area ensonified at a pulse rate of 4 pulses per second.

cSEL (dB re 1 $\mu\text{Pa}^2\cdot\text{s}$ )		No Weighting		M-Weighted							
				LF Cetaceans		MF Cetaceans		HF Cetaceans		Pinnipeds	
		Area (km <sup>2</sup> )	Radius (m)								
Injury	198	~0.009	~1.0	-	-	-	-	-	-	-	-
	192	~0.015	~1.5	-	-	~0.011	~1.5	~0.011	~1.5	-	-
	186	<0.04	<3.0	-	-	<0.02	<2.0	<0.02	<2.0	<0.01	<1.5
	179	N/A	N/A								
Behavioral Modification	183	0.011	1.5	-	-	0.009	1.0	0.009	1.0	-	-
	171	N/A	N/A								

Injury: 198 dB re 1  $\mu\text{Pa}^2\cdot\text{s}$  = mid-frequency (MF) cetaceans; 192 dB re 1  $\mu\text{Pa}^2\cdot\text{s}$  = low-frequency (LF) cetaceans; 186 dB re 1  $\mu\text{Pa}^2\cdot\text{s}$  = pinnipeds (in water); 179 dB re 1  $\mu\text{Pa}^2\cdot\text{s}$  = high-frequency (HF) cetacean.

Behavioral Modification: 183 dB re 1  $\mu\text{Pa}^2\cdot\text{s}$  = low- (LF), mid- (MF), and high-frequency (HF) cetaceans; 171 dB re 1  $\mu\text{Pa}^2\cdot\text{s}$  = pinnipeds (in water).

Dark gray shading indicates entries which are not applicable to the respective SEL threshold/M-weighting classification.

N/A – not available; requires recalculation.

Table 22. Approximate cumulative sound exposure levels for subbottom profiler, with unweighted and M-weighted radial distances and area ensonified at a pulse rate of 2 pulses per second.

cSEL (dB re 1 $\mu\text{Pa}^2\cdot\text{s}$ )		No Weighting		M-Weighted							
				LF cetaceans		MF Cetaceans		HF Cetaceans		Pinnipeds	
		Area (km <sup>2</sup> )	Radius (m)								
Injury	198	<0.01	<1.5	<0.01	<1.5	<0.01	<1.5	<0.01	<1.5	<0.01	<1.5
	192	~0.02	~2.0	~0.02	~2.0	~0.02	~2.0	~0.02	~2.0	~0.02	~2.0
	186	>0.03	>2.5	>0.03	>2.5	>0.03	>2.5	>0.03	>2.5	>0.03	>2.5
	179	>0.05	>3.0	>0.05	>3.0	>0.05	>3.0	>0.05	>3.0	>0.05	>3.0
Behavioral	183	<0.05	<3.0	<0.05	<3.0	<0.05	<3.0	<0.05	<3.0	<0.05	<3.0

Modification	171	N/A									
--------------	-----	-----	-----	-----	-----	-----	-----	-----	-----	-----	-----

Injury: 198 dB re 1  $\mu\text{Pa}^2\cdot\text{s}$  = mid-frequency (MF) cetaceans; 192 dB re 1  $\mu\text{Pa}^2\cdot\text{s}$  = low-frequency (LF) cetaceans; 186 dB re 1  $\mu\text{Pa}^2\cdot\text{s}$  = pinnipeds (in water); 179 dB re 1  $\mu\text{Pa}^2\cdot\text{s}$  = high-frequency (HF) cetaceans.

Behavioral Modification: 183 dB re 1  $\mu\text{Pa}^2\cdot\text{s}$  = low- (LF), mid- (MF), and high-frequency (HF) cetaceans; 171 dB re 1  $\mu\text{Pa}^2\cdot\text{s}$  = pinnipeds (in water).

Dark gray shading indicates entries which are not applicable to the respective SEL threshold/M-weighting classification.

N/A – not available; requires recalculation.

Table 23. Approximate cumulative sound exposure levels for subbottom profiler, with unweighted and M-weighted radial distances and area ensonified at a pulse rate of 4 pulses per second.

cSEL (dB re 1 $\mu\text{Pa}^2\cdot\text{s}$ )		No Weighting		M-Weighted							
				LF cetaceans		MF Cetaceans		HF Cetaceans		Pinnipeds	
		Area (km <sup>2</sup> )	Radius (m)								
Injury	198	~0.01	~1.5	~0.01	~1.5	~0.01	~1.5	~0.01	~1.5	~0.01	~1.5
	192	~0.03	~2.5	~0.03	~2.5	~0.03	~2.5	~0.03	~2.5	~0.03	~2.5
	186	<0.05	<3.0	<0.05	<3.0	<0.05	<3.0	<0.05	<3.0	<0.05	<3.0
	179	N/A	N/A								
Behavioral Modification	183	~0.05	~3.0	~0.05	~3.0	~0.05	~3.0	~0.05	~3.0	~0.05	~3.0
	171	N/A	N/A								

Injury: 198 dB re 1  $\mu\text{Pa}^2\cdot\text{s}$  = mid-frequency (MF) cetaceans; 192 dB re 1  $\mu\text{Pa}^2\cdot\text{s}$  = low-frequency (LF) cetaceans; 186 dB re 1  $\mu\text{Pa}^2\cdot\text{s}$  = pinnipeds (in water); 179 dB re 1  $\mu\text{Pa}^2\cdot\text{s}$  = high-frequency (HF) cetaceans.

Behavioral Modification: 183 dB re 1  $\mu\text{Pa}^2\cdot\text{s}$  = low- (LF), mid- (MF), and high-frequency (HF) cetaceans; 171 dB re 1  $\mu\text{Pa}^2\cdot\text{s}$  = pinnipeds (in water).

Dark gray shading indicates entries which are not applicable to the respective SEL threshold/M-weighting classification.

N/A – not available; requires recalculation.

---

## Discussion

---

### **5.1. Regional Effects of Environmental Parameters on Sound Propagation**

The Californian coastline spans more than 1300 km of the Pacific Ocean, between 32.5° and 42° latitude (Figure 20). The geological and oceanographic conditions are likely different in the northern and the southern coastal areas. This discussion provides an approach to assessing the applicability of the sound modeling results conducted for the central California coast region to northern and southern regions.

The degradation rate of an acoustic wave's energy (transmission loss) depends on environmental properties: bathymetry, geoacoustic properties of the sediment (bottom type), and sound speed profile in the water. The bathymetry is expected to be fairly homogeneous along the entire Californian coast, while the bottom types and the sound speed profiles change.

#### **5.1.1. Effects of Geoacoustic Properties**

An acoustic wave propagating through the water layer interacts with the ocean bottom at the water-bottom interface. As a wave reaches the interface, a fraction of the acoustic energy enters the sediment layer and the rest is reflected back into the water. The reflection coefficient of an incoming acoustic wave is the ratio of the reflected energy to the original energy.

The reflection coefficient depends on the discrepancy of acoustic impedances (defined as the product of density and sound velocity) of the media on each side of the water-bottom interface. The greater the change of acoustic properties between the media, and hence the greater the mismatch of impedances, the closer to unity the reflection coefficient is. This coefficient also depends on the incident angle of the acoustic wave; it has its minimal value when the incident angle is 90° (normal to the interface) and can reach unity at sufficiently glancing angles for certain types of interface.

The impedance of the sediment increases with increasing grain size and decreasing porosity. The sequence of the bottom type from soft to hard is: clay, silt, sand, gravel, and bedrock. For a soft bottom, the impedance is close that of water, therefore the reflection coefficient is close to zero. The transmission loss for such an environment is higher compared to harder bottom types, hence, the distances for the specific threshold levels tend to be smaller in soft bottom environments. Conversely, the reflection coefficient for a hard bottom is high. A greater amount of acoustic energy is reflected back into the water column. The transmission loss for such an environment is lower than for soft bottom types, hence, the distances to the specific threshold levels tend to be greater in harder bottom environments.

The Californian coast is classified as an active continental margin. The age of the oceanic crust at the shore line is young, less than 10 million years. Consequently, the sediment cover is thin and at some places is absent with the bedrock exposed. If the unconsolidated sediment cover exists, it is expected to be predominantly coarse sediment types: sand or gravel. The tendency of the specific bottom type occurrence is more pronounced perpendicular to the shore, rather than laterally. The exposed bedrock bottom type prevails in the near shore areas (1.5-2 km from the

shore or closer), while the sandy bottom is found more often at distances greater than 1.5-2 km from the shore.

The estimates for the distances to the specific threshold levels that are presented in this report were modeled using two types of bottom: sandy and exposed bedrock bottom. The bedrock bottom is characterized by a higher reflection coefficient that can significantly reduce the transmission loss of the acoustic wave and, consequently, result in longer ranges to the specific threshold levels.

Two sources, the boomer and the side-scan sonar, were modeled for both types of environments, while the other three sources are modeled for only the sandy-bottom environment. The exposed bedrock environment effectively doubled the distances to the specific threshold levels for the boomer source (80–120% increase), while it had virtually no effect on the acoustic field from the side-scan sonar (less than 4% increase). The latter findings can be explained by the fact that the side-scan sonar has the beam axis aligned at 5° below the horizontal plain. The acoustic wave emitted at near horizontal angles has little interaction with the bottom, therefore the geoacoustic properties of the bottom has little effect on the transmission loss for such sources. Inversely, the beam pattern of the boomer source is such that a significant amount of the acoustic energy is directed downwards. In the harder bottom environment a greater fraction of the downward-directed acoustic energy reflected back into the water column, elevating the overall acoustic levels.

The beam pattern for the single beam echosounder, multibeam echosounder, and sub-bottom profiler are similar to the boomer beam pattern. The distances to the specific threshold levels for the single beam echosounder, multibeam echosounder, and sub-bottom profiler are expected to increase similarly to the boomer source in an exposed bedrock environment.

Based on previous work conducted by JASCO (e.g., Zikov et al. 2012), it can be estimated that for the high frequency sources (e.g., single beam and multibeam echosounders) the substitution of the sandy bottom with bedrock significantly increases the distances to the specific threshold levels that were originally found in the 200–1000 m range from the source. At longer ranges, the decrease of the transmission loss due to a more reflective bottom type is compensated by the energy loss due to absorption in the sea water (about 10 dB per km for an acoustic wave at 50 kHz and 20–25 dB per km at 100 kHz). For all sources, the thresholds to the 190, 180, and 160 dB re 1  $\mu$ Pa rms SPL can likely be found up to 2.5 times farther away from the source than reported for the sandy-bottom environment, if the source is positioned above the exposed bedrock.

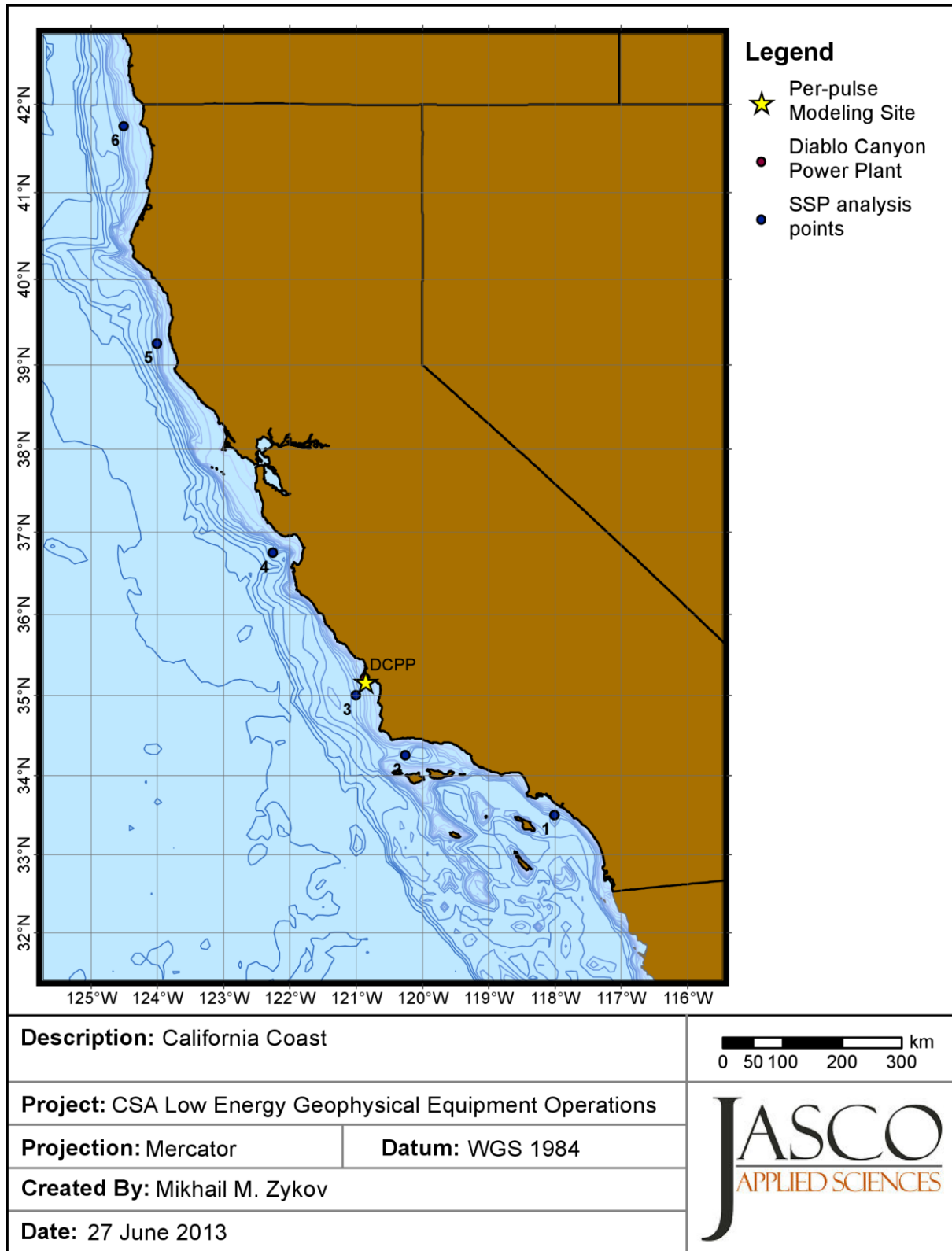


Figure 20. The sound speed profile analysis locations along the Californian coastline.

### 5.1.2. Effects of the Sound Speed Profile

The sound speed variation in the water column defines how an acoustic wave refracts. A positive sound velocity gradient near the sea surface can form a surface sound channel. Acoustic energy trapped in a surface sound channel propagates without interacting with the ocean bottom, significantly reducing transmission loss and increasing distances to specific threshold levels. Conversely, a negative sound speed gradient refracts the acoustic wave toward the ocean bottom, increasing transmission loss and decreasing distances to the specific threshold levels.

The speed of sound in the water depends primarily on three factors: pressure, water temperature, and salinity. The latter two parameters can vary spatially, as well as seasonally. The spatial and seasonal variation of the sound speed profile in the Californian coastal water column was obtained by analyzing monthly profiles from the GDEM database (Teague et al. 1990) at six sample locations (Figure 20). The general pattern of seasonal variation is virtually the same for all locations: the profile is less downwardly refracting between January and March and the strongest negative speed gradient is between September and October. The downward refracting properties of the sound speed profile decrease moving from south to north along the coast: the largest difference between the minimum and maximum speed in the sound speed profile is at the most southern location, about 30 m/s, while the lowest difference at the most northern location, about 15 m/s.

No change associated with the variation of the sound speed profiles is expected in the different locations (northern and southern) for the modeled ranges to the 190, 180, and 160 dB re 1  $\mu$ Pa root-mean-square (rms) sound pressure level (SPL) for all modeled acoustic sources, as these ranges are located close to the source and at such distances the influence of the sound speed profile on the sound propagation is minimal. The ranges to the threshold levels that are greater than 1,000 m for the modeled environment may increase by 10–20% when the sound speed profiles characteristic for the northern California coast are modeled.



---

## Literature Cited

---

- Aerts, L., M. Blee, S. Blackwell, C. Greene, K. Kim, D. Hannay, and M. Austin. 2008. *Marine mammal monitoring and mitigation during BP Liberty OBC seismic survey in Foggy Island Bay, Beaufort Sea, July-August 2008: 90-day report*. LGL Report P1011-1. Prepared by LGL Alaska Research Associates Inc., LGL Ltd., Greeneridge Sciences Inc. and JASCO Applied Sciences Ltd. for BP Exploration Alaska.
- Airmar. 2008. Technical Data Catalog. Document #17-278-259 rev. 02.
- Buckingham, M.J. 2005. Compressional and shear wave properties of marine sediments: Comparisons between theory and data. *J. Acoust. Soc. Am.* 117(1):137-152.
- Collins, M.D. 1993. A split-step Padé solution for the parabolic equation method. *J. Acoust. Soc. Am.* 93(4):1736-1742.
- Collins, M.D., R.J. Cederberg, D.B. King, and S.A. Chin-bing. 1996. Comparison of algorithms for solving parabolic wave equations. *J. Acoust. Soc. Am.* 100:178-182.
- Coppens, A.B. 1981. Simple equations for the speed of sound in Neptunian waters. *J. Acoust. Soc. Am.* 69(3):862-863.
- Endris, C. and H.G. Greene. 2011. *Potential Marine Benthic Habitats (Block 54). Seabed Classification Map Series of the Central California Continental Shelf offshore of the Diablo Canyon Power Plant*. Prepared for Pacific Gas and Electric Company.
- Fisher, F.H. and V.P. Simmons. 1977. Sound absorption in sea water. *J. Acoust. Soc. Am.* 62(3):558-564.
- Funk, D., D. Hannay, D. Ireland, R. Rodrigues, and W. Koski (eds.). 2008. *Marine Mammal Monitoring and Mitigation during Open Water Seismic Exploration by Shell Offshore Inc. in the Chukchi and Beaufort Seas, July–November 2007: 90-Day Report*. LGL Report P969-1. Prepared by LGL Alaska Research Associates Inc., LGL Ltd., and JASCO Research Ltd. for Shell Offshore Inc., National Marine Fisheries Service (US), and US Fish and Wildlife Service.  
[http://www-static.shell.com/static/usa/downloads/alaska/shell2007\\_90-d\\_final.pdf](http://www-static.shell.com/static/usa/downloads/alaska/shell2007_90-d_final.pdf).
- Hannay, D.E. and R.G. Racca. 2005. *Acoustic Model Validation*. Document Number: 0000-S-90-04-T-7006-00-E. Revision 02. Technical report for Sakhalin Energy Investment Company Ltd. by JASCO Research Ltd.  
[http://www.sakhalinenergy.com/en/documents/doc\\_33\\_jasco.pdf](http://www.sakhalinenergy.com/en/documents/doc_33_jasco.pdf).
- Hydro International. 2010. Product Survey: Side-scan Sonar Systems.
- Ireland, D.S., R. Rodrigues, D. Funk, W. Koski, and D. Hannay. 2009. *Marine mammal monitoring and mitigation during open water seismic exploration by Shell Offshore Inc. in the Chukchi and Beaufort Seas, July–October 2008: 90-day report*. LGL Report P1049-1. Prepared by LGL Alaska Research Associates Inc., LGL Ltd., and JASCO Applied Sciences for Shell Offshore Inc., Nat. Mar. Fish. Serv. (US), and US Fish and Wild. Serv. 277 p.
- ITC. 1993. *Application Equations for Underwater Sound Transducers* (pamphlet). International Transducer Corporation, Santa Barbara, CA.
- Kinsler, L.E., A.R. Frey, A.B. Coppens, and J.V. Sanders. 1950. *Fundamentals of Acoustics*. John Wiley & Sons Inc., New York.
- L-3 Klein Associates, Inc. 2010. Klein System 3000: Digital Side-scan Sonar. Product brochure.  
[http://www.l-3klein.com/wp-content/uploads/2008/05/Klein\\_System3000\\_Sep10.pdf](http://www.l-3klein.com/wp-content/uploads/2008/05/Klein_System3000_Sep10.pdf)
- Martin, B., J. MacDonnell, N. Chorney, and D. Zeddies. 2012. Sound Source Verification of Fugro Geotechnical Sources. (Appendix A) In: ESS Group, Inc. *Renewal Application for Incidental Harassment Authorization for the Non-Lethal Taking of Marine Mammals Resulting from Pre-Construction High Resolution Geophysical Survey*. For Cape Wind Associates, LLC.  
[http://www.nmfs.noaa.gov/pr/pdfs/permits/capewind\\_iha\\_application\\_renewal.pdf](http://www.nmfs.noaa.gov/pr/pdfs/permits/capewind_iha_application_renewal.pdf)
- Massa, D.P. 2003. Acoustic Transducers. In: *Wiley Encyclopedia of Telecommunications*. John Wiley & Sons, Inc.  
<http://dx.doi.org/10.1002/0471219282.eot136>.

- Nedwell, J.R. and A.W. Turnpenny. 1998. The use of a generic frequency weighting scale in estimating environmental effect. *In: Workshop on Seismics and Marine Mammals*. 23–25th June, London, U.K.
- Nedwell, J.R., A.W.H. Turnpenny, J. Lovell, S.J. Parvin, R. Workman, and J.A.L. Spinks. 2007. *A validation of the dB(ht) as a measure of the behavioural and auditory effects of underwater noise*. Report No. 534R1231 prepared by Subacoustech Ltd. for the UK Department of Business, Enterprise and Regulatory Reform under Project No. RDCZ/011/0004.  
[www.subacoustech.com/information/downloads/reports/534R1231.pdf](http://www.subacoustech.com/information/downloads/reports/534R1231.pdf).
- NGDC. 2003. U.S. Coastal Relief Model. National Geophysical Data Centre, National Oceanic and Atmospheric Administration, US Department of Commerce. <http://www.ngdc.noaa.gov/mgg/coastal/crm.html>.
- O’Neill, C., D. Leary, and A. McCrodon. 2010. Sound Source Verification. (3) *In: Blee, M.K., K.G. Hartin, D.S. Ireland, and D. Hannay (eds.). Marine mammal monitoring and mitigation during open water seismic exploration by Statoil USA E&P Inc. in the Chukchi Sea, August-October 2010: 90-day report*. LGL Report P1119. Prepared by LGL Alaska Research Associates Inc., LGL Ltd., and JASCO Applied Sciences Ltd. for Statoil USA E&P Inc., National Marine Fisheries Service (US), and US Fish and Wildlife Service. pp 3-1 to 3-34.
- Porter, M.B. and Y.-C. Liu. 1994. Finite-element ray tracing. *In: Lee, D. and M.H. Schultz (eds.). Proceedings of the International Conference on Theoretical and Computational Acoustics*. Volume 2. World Scientific Publishing Co. pp 947-956.
- R2Sonic. 2011. Sonic 2024/2022 Broadband Multibeam Echosounders: Operation Manual V3.1.
- R2Sonic. 2012. Sonic 2020/2022/2024 Product brochure.  
[http://www.r2sonic.com/pdfs/R2Sonic\\_Product\\_Brochure.pdf](http://www.r2sonic.com/pdfs/R2Sonic_Product_Brochure.pdf)
- Simpkin, P.G. 2005. The boomer sound source as a tool for shallow water geophysical exploration. *Marine Geophys. Res.* 26, pp. 171-181.
- Southall, B.L., A.E. Bowles, W.T. Ellison, J.J. Finneran, R.L. Gentry, C.R. Greene Jr., D. Kastak, D.R. Ketten, J.H. Miller, et al. 2007. Marine mammal noise exposure criteria: Initial scientific recommendations. *Aquatic Mammals*. 33(4):411-521.
- Teague, W.J., M.J. Carron, and P.J. Hogan. 1990. A Comparison Between the Generalized Digital Environmental Model and Levitus Climatologies. *J. Geophys. Res.* 95(C5):7167-7183.
- Verbeek, N.H. and T.M. McGee. 1995. Characteristics of High-resolution marine reflection profiling sources. *J. Appl. Geophys.* 33:251-269.
- Warner, G., C. Erbe, and D. Hannay. 2010. Underwater sound measurements. (Chapter 3) *In: Reiser, C.M., D.W. Funk, R. Rodrigues, and D. Hannay (eds.). Marine mammal monitoring and mitigation during open water seismic exploration by Shell Offshore Inc. in the Alaskan Chukchi Sea, July-October 2009: 90-day report*. LGL Alaska Research Associates Inc. and JASCO Applied Sciences for Shell Offshore Inc., Nat. Mar. Fish. Serv. (US), and US Fish and Wild. Serv.
- Zykov, M., M.-N.R. Matthews, and N.E. Chorney. 2012. Underwater Noise Assessment: Central Coastal California Seismic Imaging Project. JASCO Document 00271, Version 3.0. Technical report for Environmental Resources Management by JASCO Applied Sciences.